NEW MAXIMAL SURFACES IN MINKOWSKI 3-SPACE WITH ARBITRARY GENUS AND THEIR COUSINS IN DE SITTER 3-SPACE

SHOICHI FUJIMORI, WAYNE ROSSMAN, MASAAKI UMEHARA, KOTARO YAMADA, AND SEONG-DEOG YANG

Dedicated to the memory of Professor Katsumi Nomizu

Abstract. Until now, the only known maximal surfaces in Minkowski 3-space of finite topology with compact singular set and without branch points were either genus zero or genus one, or came from a correspondence with minimal surfaces in Euclidean 3-space given by the third and fourth authors in a previous paper. In this paper, we discuss singularities and several global properties of maximal surfaces, and give explicit examples of such surfaces of arbitrary genus. When the genus is one, our examples are embedded outside a compact set. Moreover, we deform such examples to CMC-1 faces (mean curvature one surfaces with admissible singularities in de Sitter 3-space) and obtain "cousins" of those maximal surfaces.

Cone-like singular points on maximal surfaces are very important, although they are not stable under perturbations of maximal surfaces. It is interesting to ask if cone-like singular points can appear on a maximal surface having other kinds of singularities. Until now, no such examples were known. We also construct a family of complete maximal surfaces with two complete ends and with both cone-like singular points and cuspidal edges.

Introduction

Maximal surfaces in the Minkowski 3-space $\boldsymbol{R}^3_1$ arise as solutions of the variational problem of locally maximizing the area among spacelike surfaces. By definition, they have everywhere vanishing mean curvature. Like the case of minimal surfaces in Euclidean 3-space, maximal surfaces possess a Weierstrass-type representation formula [18].

The most significant difference between minimal and maximal surfaces is the fact that the only complete spacelike maximal surfaces are planes [2, 3], which is probably the main reason why people have not paid much attention to maximal surfaces. If we allow some sorts of singular points for maximal surfaces, however, the situation changes. Osamu Kobayshi [19] investigated cone-like singular points on maximal surfaces. After that, many interesting examples with cone-like singular points have been found and studied by F. J. López, R. López, and Souam [24], Fernández and F. J. López [6], and Fernández, F. J. López and Souam [7], Fernández [5] and others.

Date: October 15, 2009.

2000 *Mathematics Subject Classification.* Primary 53A10; Secondary 53A35, 53C50.

Key words and phrases. maximal surfaces, CMC-1 surfaces in de Sitter space, singularities.

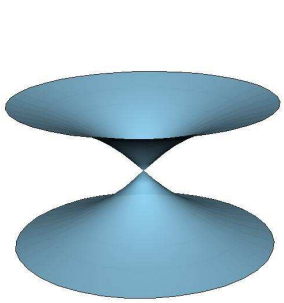

the Lorentzian catenoid,
$(G, \eta) = (z, dz/z^2)$ on $\boldsymbol{C} \setminus \{0\}$

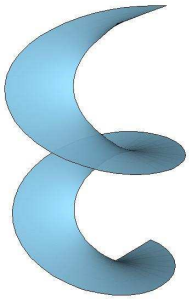

the Lorentzian helicoid,
$(G, \eta) = (z, i\, dz/z^2)$
on the universal cover of $\boldsymbol{C} \setminus \{0\}$

FIGURE 1. The duality between cone-like singular points and fold singular points. The pair (G, η) denotes the Weierstrass data, see Section 1.

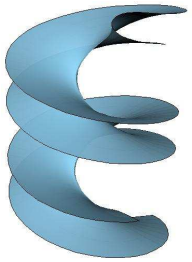

FIGURE 2. An associated surface of the Lorentzian helicoid, with Weierstrass data $(G, \eta) = (z, e^{\pi i/4} z^{-2} dz)$.

On the other hand, for the study of more general singularities, Estudillo and Romero [4] initially defined a class of maximal surfaces with singular points of more general type, and investigated criteria for such surfaces to be planes. Recently, Imaizumi [15] studied the asymptotic behavior of maximal surfaces, and Imaizumi-Kato [16] gave a classification of maximal surfaces of genus zero with at most three embedded ends. In [32], the third and forth authors showed that if admissible singular points are included, then there is an interesting class of objects called *maxfaces*. In fact, the three surface classes

- non-branched generalized maximal surfaces in the sense of [4],
- non-branched generalized maximal maps in the sense of [16], and
- maxfaces in the sense of [32]

are all the same class of maximal surfaces. So in this paper, we shall call such a class of surfaces *maxfaces*. Maxfaces are spacelike at their regular points, but the limiting tangent plane (that is, the Lorentzian orthogonal complement of the normal vector) at each singular point contains a lightlike direction. For the global study of maximal surfaces, the following terminology given in [32] is useful:

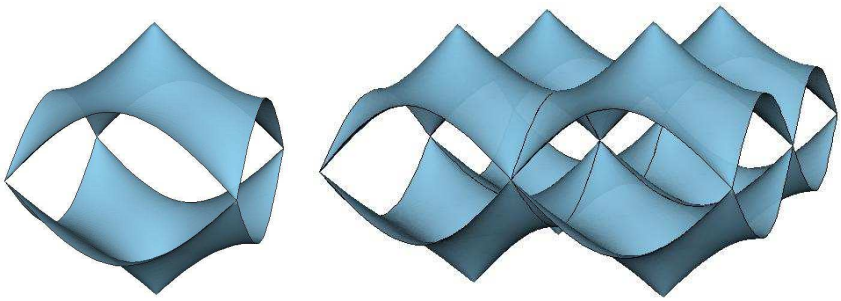

FIGURE 3. A weakly complete triply-periodic maxface with cone-like singular points corresponding to the Schwarz-P surface; see [13] for details.

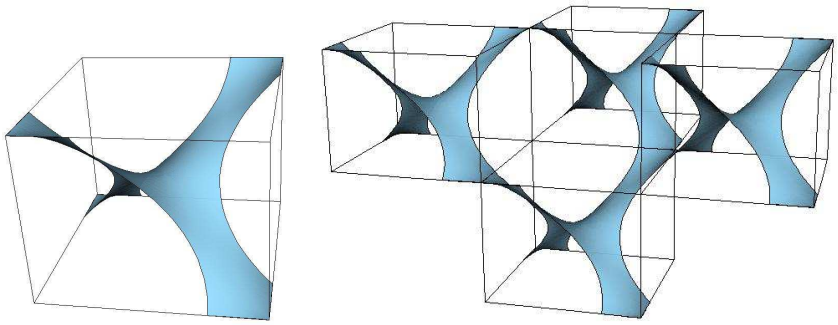

FIGURE 4. A weakly complete triply-periodic maxfaces with fold singular points corresponding to the Schwarz-D surface; see [13] for details.

Definition I. A maxface (or more generally, a generalized maximal surface) $f\colon M \to \boldsymbol{R}^3_1$ is called *complete* if there exists a symmetric 2-tensor T which vanishes outside a compact set in M, such that $ds^2 + T$ is a complete Riemannian metric on M, where ds^2 is the induced metric by f. If f is complete, the set of singular points is compact in M. On the other hand, a maxface is called *weakly complete* (in the sense of [32]), if its null holomorphic lift into $\boldsymbol{C}^3$ (see Section 1) has complete induced metric with respect to the canonical Hermitian metric on $\boldsymbol{C}^3$.

As shown in [32, Lemma 4.3], completeness implies weak completeness. Conversely, *a weakly complete maxface is complete if and only if the singular set is compact and each end is conformally equivalent to a punctured disc* (see [33]). A typical well-known complete maxface is the Lorentzian catenoid (see [18], see also [1] in which it is called the *Lorentzian elliptic catenoid*; Figure 1, left), which has a *cone-like singular point* (see Section 2 for the definition). Like minimal surfaces in Euclidean 3-space $\boldsymbol{R}^3$, maxfaces have conjugate surfaces. A cone-like singular point on a maxface corresponds to a fold singular point on its conjugate maxface, in general. For the proof of this and the definition of fold singular points, see [23]. The Lorentzian helicoid (see [18], see also [1]; Figure 1, right) is weakly complete

(but not complete) and is the conjugate maxface of the Lorentzian catenoid, whose image consists of two surfaces with 'boundary' in $\boldsymbol{R}^3_1$. The boundary (that is, the singular set) is a helix, and each interior image point on the surface has two inverse images. Namely, the Lorentzian helicoid can be regarded as a fold along a helix.

As shown in [14], generic singular points of maxfaces are cuspidal edges, swallowtails and cuspidal cross caps. Thus, cone-like singular points and folds are non-generic. For example, one can consider an isometric deformation of Lorentzian helicoid corresponding to the family of Weierstrass data $(z, e^{it}dz/z^2)$ $(t \in [0, \pi/2])$. Figure 2 gives the maxface corresponding $t = \pi/4$, whose singular points consist only of cuspidal edges.

However, they (i.e., cone-like singular points and folds) are important singular points in the theory of maxfaces. For example, fold singular points (i.e., the double surfaces in [16]) appear under a certain situation, see [16, Proposition 7.7 and Page 581].

It should be remarked that a complete maxface automatically has finite total curvature outside of a compact set, and finite topology as well (see [32, Theorem 4.6 and Corollary 4.8]). This is a property that is crucially different from the case of minimal surfaces in $\boldsymbol{R}^3$. So, interestingly, there are no complete periodic maxfaces although there exist compact maxfaces in a Lorentzian torus $\boldsymbol{R}^3_1/\Gamma$ for a suitable lattice (namely, triply-periodic weakly complete maxface in $\boldsymbol{R}^3_1$). In fact, the same Weierstrass data as for the Schwarz P-surface and the Schwarz D-surface give such examples. See Figures 3 and 4.

In [32, Theorem 4.11], it was shown that an Osserman-type inequality

$$2\deg G \geq -\chi(M) + (\text{number of ends}) \tag{1}$$

holds for the degree of the Gauss map of complete maxfaces $f : M \to \boldsymbol{R}^3_1$, and equality holds if and only if all ends are properly embedded. Here

$$G : M \longrightarrow S^2 = \boldsymbol{C} \cup \{\infty\}$$

is the Lorentzian Gauss map and $\deg G$ is its degree as a map to the hyperbolic sphere S^2 considered as a compactification of the hyperboloid in $\boldsymbol{R}^3_1$, see [32] and [20, Section 5]. Since G is meromorphic at each end of a complete maxface, the left-hand side of (1) is finite (see Fact 1.2).

In [12], the authors showed that a similar Osserman-type inequality (1) also holds for the hyperbolic Gauss maps G of complete CMC-1 faces in de Sitter 3-space (for the definition of CMC-1 faces, see Section 4). In contrast to the case of maxfaces, the hyperbolic Gauss map of a CMC-1 face may have an essential singularity at an end.

The Lorentzian catenoid satisfies equality in (1). In [32], several examples which attain equality in (1) were given. Recently, complete maxfaces with three embedded ends were classified by Imaizumi and Kato [16]. We mention here two new interesting phenomena on the shape of singular points on maximal surfaces:

Example 1. (Trinoids whose graphics seem to show cone-like singular points, although no cone-like singularities exist). We set

$$M = \boldsymbol{C} \setminus \{a, -a\} \qquad (a > 1/2)$$

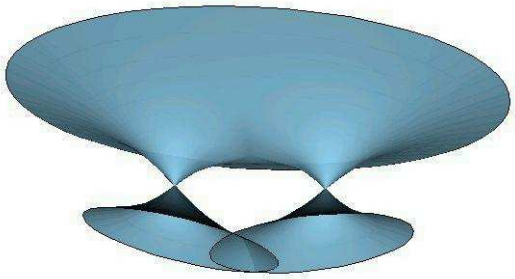

Trinoid in (2) for $a = 3.67$

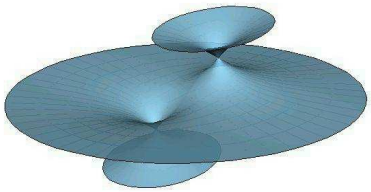

Trinoid in (3) for $c = 0.1$

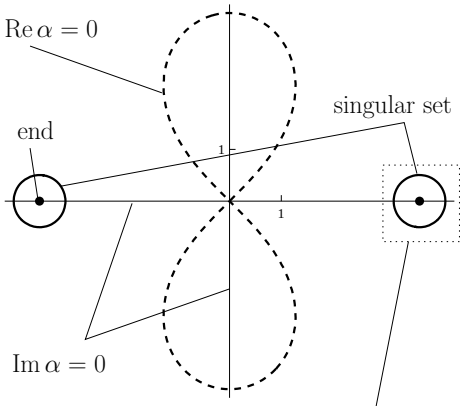

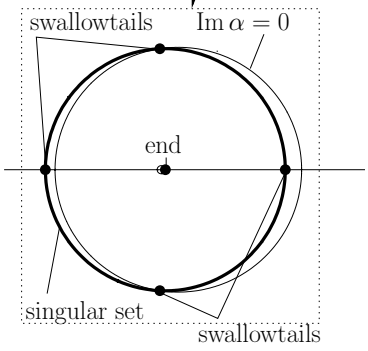

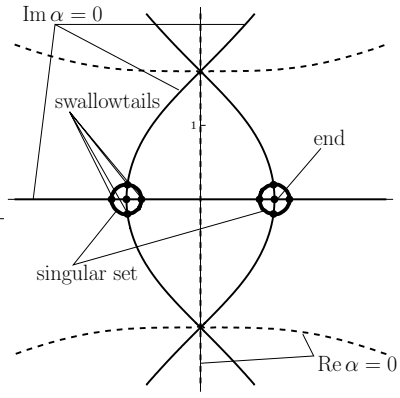

Singular set of (2) for $a = 3.67$

Singular set of (3) for $c = 0.1$

Both trinoids have eight swallowtails and cuspidal edges for singular points. No cuspidal cross caps appear. For the notations, see Section 1.

FIGURE 5. The trinoids in Example 1.

and consider two Weierstrass data (see Section 1)

$$G := \frac{b - z^2}{z}, \qquad \eta := \frac{z^2 dz}{(z^2 - a^2)^2} \qquad \left(b := -a^2 + a\sqrt{4a^2 - 1}\right). \tag{2}$$

Substituting these into (1.4), we get a trinoid with three embedded ends at $z = \pm a, \infty$, each of which is asymptotic to a Lorentzian catenoid. The left-hand figure in Figure 5 shows the image with $a = 3.67$.

On the other hand, set

$$M = \boldsymbol{C} \setminus \{1, -1\}, \qquad G = c\frac{z^2 + 3}{z^2 - 1}, \quad \text{and} \quad \eta = \frac{dz}{c} \qquad (c > 0, c \neq 1). \tag{3}$$

Then we have another trinoid as in Figure 5, right. The ends 1, -1 are asymptotic to the Lorentzian catenoid, and the end ∞ to the plane. The figure shows the image for $c = 0.1$.

Since a maxface is symmetric with respect to a given cone-like singular point (cf. [16] and [23]), neither of these two maxfaces admits any cone-like singular points.

However, in Figure 5, we can see two singular sets in each surface which look very much like cone-like singularities. The singular sets do, however, consist of cuspidal edges and swallowtails (see Figure 5).

Similarly, there are four cuspidal cross caps on the Enneper maxface (see [32, Example 5.2]). However, it is difficult to recognize the crossing of two sheets on surfaces near these four singular points from computer graphics, since these two sheets are so close to each other. If a maxface admits a cone-like singular point (resp. a swallowtail), its conjugate surface admits fold singular points (resp. a cuspidal cross cap) and vice versa ([23] and [14, Corollary 2.5]; for the definition of cone-like singular points, see Definition 2.1). Thus, in computer graphics, the fact that a union of swallowtails sometimes look like cone-like singular points and the fact that cuspidal cross caps look like fold singular points seems to be a mutually dual phenomena. The authors hope that one could establish a new theory for explaining this. In recent private conversations, Shin Kato [17] said that this phenomenon for trinoids as in Figure 5 seems to occur as a family of trinoids "collapses" to Lorentzian catenoids (which have a cone-like singularity).

It is interesting to ask if there exist maxfaces having a cone-like singular point and also having singular points which are not cone-like. We give such an example:

Theorem A. *There exists a maxface $f\colon M \to \boldsymbol{R}^3_1$ of genus 0 with two complete ends whose singular set in M consists of cone-like singular points, cuspidal edges, swallowtails, and cuspidal cross caps. Here, the image of the cone-like singular points is a single point.*

The proof of the first part of this theorem is given in Section 2.

In $\boldsymbol{R}^3$, examples of complete embedded minimal surfaces of finite total curvature of course are known — for example, the plane, the catenoid, the Costa surface, the Costa-Hoffman-Meeks surface, etc. As a related class of maxfaces, the authors give here the following:

Definition II. A complete maxface is called *embedded* (*in the wider sense*) if it is embedded outside of some compact set of $\boldsymbol{R}^3_1$.

From here on out, when we use the word "embedded" for a maxface, we always mean "embedded in the wider sense" as in the above definition. By definition, an embedded maxface attains equality in (1). In a joint work [22] with Kim, the fifth author constructed maximal surfaces of genus $k = 1, 2, 3, \ldots$, which are complete generalized maximal surfaces in the sense of [4] (i.e., they admit branch points when $k \geq 2$), and when $k = 1$ it is a complete embedded maxface, see Figure 6. We shall call this example the *Kim-Yang toroidal maxface*. We remark that there exist no embedded minimal surface in $\boldsymbol{R}^3$ with two ends except the catenoid (cf. [29]).

Until now, the only known examples of embedded complete maxfaces were

- the spacelike plane (which is the only example of a complete maximal surface without singular points),
- the Lorentzian catenoid,
- the Kim-Yang toroidal maxface.

Also, until now the only known complete positive-genus maxfaces were the Lorentzian Chen-Gackstatter surface (given in [32, Example 5.5]) and the Kim-Yang toroidal maxface. In this article, we construct complete maxfaces with two ends and arbitrary genus, which are embedded if the genus is equal to 1. (Theorem B).

On the other hand, surfaces of constant mean curvature one (CMC-1 surfaces) in de Sitter 3-space S^3_1 have similar properties to maximal surfaces in $\boldsymbol{R}^3_1$ (cf. [8] and [12]). Analogous to maxfaces, a notion of CMC-1 faces in S^3_1, which is CMC-1 surfaces with certain kinds of singular points, was introduced in [8]. Related to this, the second, the third and forth authors introduced in [27] a method to deform minimal surfaces in $\boldsymbol{R}^3$ to CMC-1 surfaces in hyperbolic 3-space. In this paper, we demonstrate that this method works for maxfaces in $\boldsymbol{R}^3_1$ and CMC-1 faces in S^3_1 as well (see Section 4 and the appendix).

In this article, we shall prove:

Theorem B. *There exists an family of complete maxfaces f_k for $k = 1, 2, 3, \ldots$ with two ends, and of genus k if k is odd and genus $k/2$ if k is even. Moreover, f_1 and f_2 are embedded (in the wider sense). Furthermore, the number of swallowtails and the number of cuspidal cross caps are both equal to $4(k+1)$ if k is odd and $2(k+1)$ if k is even. In particular, f_1 and f_2 are both of genus one, but are not congruent. (Compare Figures 6 and 9.)*

Moreover, such maxfaces f_k can be deformed to complete CMC-1 faces in S^3_1, which are embedded (in the wider sense) if $k = 1$ or 2.

We note that f_1 is the Kim-Yang toroidal maxface, but the f_k are new examples for all $k \geq 2$. The proof of this theorem is given in Sections 3 and 4. The method of construction is somewhat similar to that of [22], but one salient feature of our new family is that it is free of branch points for all $k = 1, 2, 3, \ldots$, whereas the surfaces in the corresponding family of [22] have two branch points whenever $k \geq 2$. However, there is still a scarcity of examples of complete maxfaces, especially embedded examples.

In light of the relationships between maxfaces and CMC-1 faces, we give a pair of open problems about finding new surfaces:

Problem 1. *Are there complete maxfaces (resp. complete CMC-1 faces) with embedded ends of genus greater than one in $\boldsymbol{R}^3_1$ (or S^3_1)? Furthermore, could such examples actually be embedded (in the wider sense)?*

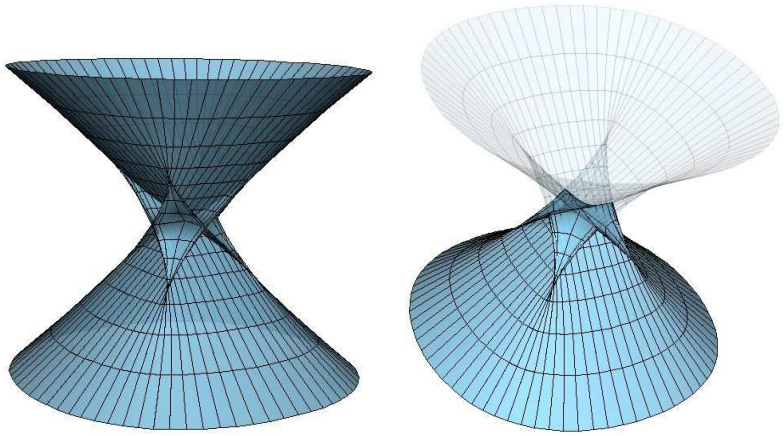

FIGURE 6. The example for $k = 1$ (Kim-Yang toroidal maxface) and half of it.

The first and second authors [11] provided numerical evidence for the existence of CMC-1 faces in S^3_1 of higher genus with two embedded ends.

Problem 2. *Are there complete maxfaces* (*resp. complete CMC*-1 *faces*) *with more than two ends of positive genus in* $\boldsymbol{R}^3_1$ (*or* S^3_1)*?*

The present state of this field is such that it would be very beneficial to have a larger collection of examples, as described in these open problems, for example. A number of types of maximal surfaces can be produced from a canonical correspondence with minimal surfaces in Euclidean 3-space given in Section 5 of [32] (for example, this method applies to the minimal surfaces of arbitrary genus found in [28]), although this construction needs to solve a period problem. (Correspondence of minimal surfaces and maximal surfaces was first introduced in [2] for graphs.)

Non-orientable complete maxfaces were recently found in a joint work [10] of the first author with López. (Unfortunately, the ends of these examples are not embedded.) On the other hand, CMC-1 faces in S^3_1 are all orientable (this fact is not trivial, since the surface admits singular points, see [20]). Weakly complete (but not complete) bounded maxfaces (resp. CMC-1 faces) with arbitrary genus were constructed in [25] and [26].

Acknowledgements. The authors thank Shin Kato for valuable conversations. The third and fourth authors also thank Francisco J. López for valuable conversations during their stay at Granada.

1. Preliminaries

In this section, we review the Weierstrass-type representation formula for maxfaces (see [18, 32]), and criteria for singular points (see [32, 14]).

Throughout this paper, we denote by $\boldsymbol{R}^3_1$ the Minkowski 3-space with the inner product $\langle\ ,\ \rangle$ of signature $(-,+,+)$.

Fact 1.1 ([32, Theorem 2.6])**.** *Let M be a Riemann surface with a base point $o \in M$, and (G, η) a pair of a meromorphic function and a holomorphic 1-form on M such*

that

$$(1+|G|^2)^2|\eta|^2 \tag{1.1}$$

gives a (positive definite) Riemannian metric on M, and $|G|$ is not identically 1. Let

$$\Phi := \big(-2G, 1+G^2, i(1-G^2)\big)\eta \tag{1.2}$$

and assume

$$\operatorname{Re}\oint_{\gamma_j}\Phi = 0 \qquad (j=1,\dots,N), \tag{1.3}$$

for loops $\{\gamma_j\}_{j=1}^N$ such that the set $\{[\gamma_j]\}$ of homotopy classes generates the fundamental group $\pi_1(M)$ of M. Then

$$f(p) := \operatorname{Re}\int_o^p \Phi = \operatorname{Re}\int_o^p \big(-2G, 1+G^2, i(1-G^2)\big)\eta \tag{1.4}$$

is well-defined on M and gives a maxface in $\boldsymbol{R}^3_1$. Moreover, any maxfaces are obtained in this manner. The induced metric ds^2 and the second fundamental form $\mathrm{I\!I}$ are expressed as

$$ds^2 = \big(1-|G|^2\big)^2|\eta|^2 \quad \textit{and} \quad \mathrm{I\!I} = Q+\overline{Q}, \qquad (Q=\eta\, dG), \tag{1.5}$$

respectively. Weak completeness as in Definition I in the introduction is equivalent to completeness of the metric (1.1). The point $p\in M$ is a singular point of the maxface (1.4) if and only if $|G(p)|=1$.

We call the pair (G,η) the *Weierstrass data* of the maxface f in (1.4), G the *Lorentzian Gauss map*, and the holomorphic 2-differential Q in (1.5) the *Hopf differential*, respectively.

Fact 1.2 ([33])**.** *Let M be a Riemann surface, and $f\colon M\to \boldsymbol{R}^3_1$ a weakly complete maxface. Then f is complete if and only if there exists a compact Riemann surface $\overline{M}$ and a finite number of points $p_1,\dots,p_n\in\overline{M}$ such that M is conformally equivalent to $\overline{M}\setminus\{p_1,\dots,p_n\}$, and the set of singular points*

$$\Sigma = \{p\in M\,;\,|G(p)|=1\}$$

is compact. In this case, the Weierstrass data (G,η) is well-defined as a pair of a meromorphic function and a meromorphic one form on $\overline{M}$, and the compactness of the singular set Σ is equivalent to the condition $|G(p_j)|\neq 1$ for $j=1,\dots,n$.

As shown in [14], generic singular points of maxfaces (resp. CMC-1 faces) are cuspidal edges, swallowtails and cuspidal cross caps. We recall criteria for generic singular points of maxfaces. For terminology on CMC-1 faces, see Section 4.

Fact 1.3 ([32, Theorem 3.1], [14, Theorem 2.4])**.** *Let U be a domain of the complex plane $(\boldsymbol{C},z)$ and $f: M\to\boldsymbol{R}^3_1$ a maxface, (G,η) its Weierstrass data. Set*

$$\alpha := \frac{dG}{G^2\eta}, \quad \textit{and} \quad \beta := G\frac{d\alpha}{dG} \tag{1.6}$$

Then

1. *A point $p\in M$ is a singular point of f if and only if $|G(p)|=1$.*
2. *f is right-left equivalent to a cuspidal edge at p if and only if $\operatorname{Im}\alpha(p)\neq 0$,*

(3) *f is right-left equivalent to a swallowtail at p if and only if* $\operatorname{Im}\alpha(p) = 0$ *and* $\operatorname{Re}\beta(p) \neq 0$,
(4) *and f is right-left equivalent to a cuspidal cross cap at p if and only if* $\operatorname{Re}\alpha(p) = 0$, $\alpha(p) \neq 0$, *and* $\operatorname{Im}\beta(p) \neq 0$.

Here, two C^∞-maps $f_1\colon (U_1, p) \to N^3$ and $f_2\colon (U_2, q) \to N^3$ of domains $U_j \subset \boldsymbol{R}^2$ $(j = 1, 2)$ into a 3-manifold N^3 are *right-left equivalent* at the points $p \in U_1$ and $q \in U_2$ if there exists a local diffeomorphism φ of $\boldsymbol{R}^2$ with $\varphi(p) = q$ and a local diffeomorphism Φ of N^3 with $\Phi(f_1(p)) = f_2(q)$ such that $f_2 = \Phi \circ f_1 \circ \varphi^{-1}$.

2. Maxfaces with cone-like singular points

In this section, we give the proof of Theorem A in the introduction. To do this, we recall a definition and a criterion for cone-like singular points.

2.1. **Cone-like singular points.**

Definition 2.1 (Cone-like singular points). Let Σ_0 be a connected component of the set of singular points of the maxface f as in (1.4) which consists of non-degenerate singular points in the sense of [32, Section 3] and [14]. Then each point of Σ_0 is called a *generalized cone-like singular point* if Σ_0 is compact and the image $f(\Sigma_0)$ is one point. Moreover, if there is a neighborhood U of Σ_0 and $f(U \setminus \Sigma_0)$ is embedded, each point of Σ_0 is called a *cone-like singular point.*

Remark 2.2. In [19] and [7], the image $f(\Sigma_0)$ as a single point of the cone-like singular points is called a *cone-like singular point*. However, we do not use this terminology here, since we treat the singular set not in $\boldsymbol{R}^3_1$ but in the source manifold.

Lemma 2.3. *A connected component Σ_0 of the set of singular points of the maxface* (1.4) *consists of generalized cone-like singular points if and only if it is compact, and*

$$\alpha \neq 0 \qquad \textit{and} \qquad \operatorname{Im}\alpha = 0$$

holds, where α is a function on M as in (1.6).

Proof. Take a complex coordinate z around $p \in \Sigma_0$ and identify the tangent plane of M with $\boldsymbol{C}$. The point p is non-degenerate if and only if $\alpha \neq 0$, because of [32, Lemma 3.3]. The singular direction (the tangential direction of the singular set) and the null direction (the direction of the kernel of df) are represented as $i\overline{(G'/G)}$ and $i/(G\hat{\eta})$, where $' = d/dz$ and $\eta = \hat{\eta}\, dz$ (see [32, Proof of Theorem 3.1]). Here, the image $f(\Sigma_0)$ consists of one point if and only if these two directions are linearly dependent. Thus we have the conclusion. □

Since $dG \neq 0$ on the set Σ_0 of generalized cone-like singular points, Σ_0 is diffeomorphic to the circle S^1.

By [7, Lemma 1], we have the following criterion:

Lemma 2.4. *Assume a connected component Σ_0 of the singular set of a maxface consists of generalized cone-like singular points. Then it consists of cone-like singular points if and only if $G|_{\Sigma_0}\colon \Sigma_0 \to S^1 \subset \boldsymbol{C}$ is injective and η does not vanish on Σ_0, where (G, η) is the Weierstrass data.*

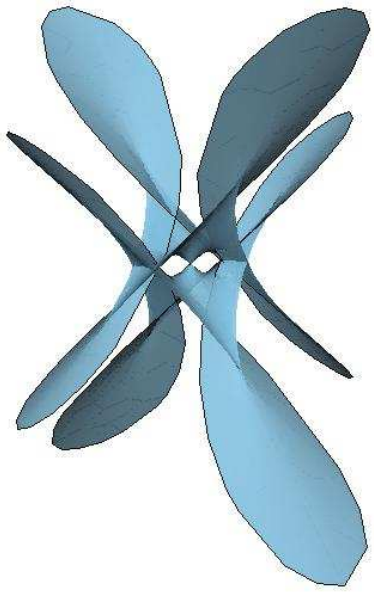

The image of the surface with (2.1) and $a = 2.5$.

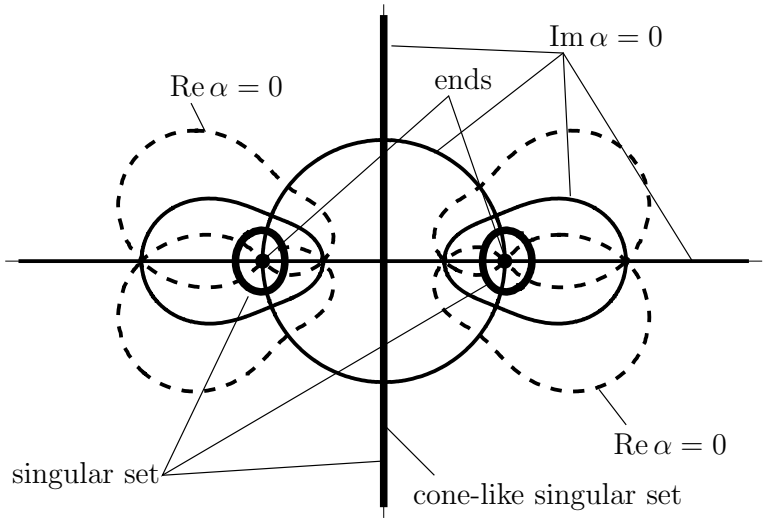

The singular set in the z-plane. The imaginary axis corresponds to the set of cone-like singular points, and the other connected components each consist of cuspidal edges, four swallowtails (the intersection points of the singular set with the curve $\operatorname{Im}\alpha = 0$, the curves shown in thin lines), and four cuspidal cross caps (the intersection points of the singular set with the curve $\operatorname{Re}\alpha = 0$, the dotted curves).

FIGURE 7. A maxface with a cone-like singularity and other singularities

2.2. **Proof of Theorem A.** Let $M := \boldsymbol{C} \cup \{\infty\} \setminus \{-1, 1\}$ and let a be a real constant such that $1 < a < 4$ and $a \neq 2$. Set

$$G = \frac{(z-1)(z^2+az+1)}{(z+1)(z^2-az+1)}, \qquad \eta = \frac{(z^2-az+1)^2}{(z-1)^4(z+1)^2}\,dz. \tag{2.1}$$

Then the data (G, η) gives no real period in the representation formula (1.4), i.e., it satisfies (1.3). Thus it defines a maxface of genus zero with 2-ends:

$$f\colon M \longrightarrow \boldsymbol{R}^3_1. \tag{2.2}$$

Since $a \in \boldsymbol{R}$, it holds that $|G| = 1$ on the imaginary axis. When $1 < a < 4$ and $a \neq 2$, the singular set $\Sigma = \{|G| = 1\}$ consists of three disjoint (topological) circles on the Riemann sphere, including the imaginary axis of the z-plane (Figure 7, bottom).

Set $\alpha := dG/(G^2\eta)$ as in Section 1. Then the set $\{\operatorname{Im}\alpha = 0\}$ looks like as in Figure 7, bottom. In particular, $\operatorname{Im}\alpha = 0$ on the imaginary axis, and hence Lemma 2.3 implies that the imaginary axis consists of generalized cone-like singular points. Here, since G is of degree 3 and the singular set consists of three connected components, G is injective on each connected component of the singular set. Since $\eta \neq 0$ on the imaginary axis, Lemma 2.4 implies that the imaginary axis consists of cone-like singular points.

On the other hand, other connected components of the singular set contain cuspidal edges, because $\operatorname{Im}\alpha$ is not identically zero on the singular set.

Since the order of the Hopf differential Q at $z = \pm 1$ is -4, both ends are Enneper ends (cf. Example 5.2 in [32]), as shown in Figure 7, top.

3. Proof of The first part of Theorem B

In this section, we construct maxfaces f_k $(k = 1, 2, 3, \dots)$ as in the statement of Theorem B. To do it, we proceed as follows for each k:

- Take a Riemann surface M_k of genus k, which is a compact Riemann surface excluding 2 points (which correspond to the ends), see Section 3.1.
- Construct a complete maxface $\hat{f}_k\colon M_k \to \boldsymbol{R}^3_1$ $(k = 1, 2, 3, \dots)$, see Sections 3.1–3.4.
- When $k = 2m$ is an even number, show that M_k is the double cover of a Riemann surface M'_k of genus m, and $\hat{f}_k$ induces a complete maxface $f_k\colon M'_k \to \boldsymbol{R}^3_1$. See Section 3.5.
- When k is odd, we set $f_k = \hat{f}_k$.

3.1. The Riemann surface M_k.

Let

$$\overline{M}_k = \left\{(z, w) \in (\boldsymbol{C} \cup \{\infty\})^2\,;\, w^{k+1} = z\left(z^2 - 1\right)^k\right\}, \tag{3.1}$$

where k is a positive integer. As a submanifold of $(\boldsymbol{C} \cup \{\infty\})^2$, $\overline{M}_k$ has singular points at $(z, w) = (\pm 1, 0)$ and (∞, ∞). However, one can define on $\overline{M}_k$ the structure of a Riemann surface using complex coordinates ζ_0, ζ_∞, ζ_1 and ζ_{-1} around $(z, w) = (0, 0)$, (∞, ∞), $(1, 0)$, and $(-1, 0)$, respectively, as follows:

$$\begin{aligned} &z = (\zeta_0)^{k+1} && \text{at } (0,0), && z = (\zeta_\infty)^{-k-1} && \text{at } (\infty,\infty),\\ &z = 1 + (\zeta_1)^{k+1} && \text{at } (1,0), && z = -1 + (\zeta_{-1})^{k+1} && \text{at } (-1,0). \end{aligned} \tag{3.2}$$

Hence the holomorphic map $z\colon \overline{M}_k \to \boldsymbol{C} \cup \{\infty\}$ is of degree $k + 1$ with total branching number $4k$. Then by the Riemann-Hurwitz relation, the genus of $\overline{M}_k$ is k.

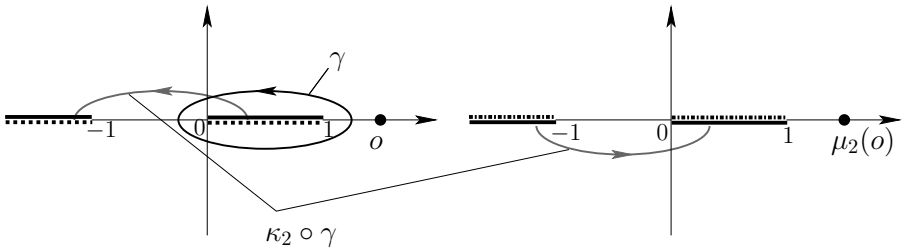

The projection of the loops γ and $\kappa_2 \circ \gamma$ to the z-plane are shown. The left-hand (resp. right-hand) figure shows the z-plane such that $\arg w = 0$ ($\arg w = 2k\lambda$) when $z > 1$.

FIGURE 8. The loops γ and $\kappa_2 \circ \gamma$.

We shall construct maxfaces $\hat{f}_k \colon M_k \to \boldsymbol{R}^3_1$ $(k = 1, 2, 3, \dots)$ with two ends corresponding to $(0, 0)$ and (∞, ∞), where

$$M_k = \overline{M}_k \setminus \{(0,0), (\infty,\infty)\}. \tag{3.3}$$

Let $\widetilde{M_k}$ be the universal cover of M_k.

3.2. **Symmetries and the fundamental group of M_k.** For simplicity, we set

$$\lambda := \frac{\pi}{k+1}. \tag{3.4}$$

Define reflections (orientation-reversing conformal diffeomorphisms) $\mu_j \colon M_k \to M_k$ $(j = 1, 2, 3, 4)$ as

$$\begin{aligned} &\mu_1(z,w) = (\bar{z}, \bar{w}), && \mu_2(z,w) = (\bar{z}, e^{2ki\lambda}\bar{w}), \\ &\mu_3(z,w) = (-\bar{z}, e^{-i\lambda}\bar{w}), && \mu_4(z,w) = \left(\frac{1}{\bar{z}}, e^{ik\lambda}\frac{\bar{w}}{\bar{z}^2}\right). \end{aligned} \tag{3.5}$$

Using these, we define the following automorphisms of M_k:

$$\begin{aligned} &\kappa_1 := \mu_2 \circ \mu_1 && \big(\kappa_1(z,w) = (z, e^{2ki\lambda}w)\big), \\ &\kappa_2 := \mu_3 \circ \mu_1 && \big(\kappa_2(z,w) = (-z, e^{-i\lambda}w)\big). \end{aligned} \tag{3.6}$$

Choose a base point $o \in M_k$ such that

$$o \in \{(t,w)\,;\, 1 < t < \infty, \arg w = 0\} \subset M_k, \tag{3.7}$$

and take a loop γ on M_k starting at o as in Figure 8. Then we have the following:

Lemma 3.1. *The fundamental group $\pi_1(M_k)$ of M_k is generated by*

$$[(\kappa_1)^j \circ \gamma] \quad \textit{and} \quad [(\kappa_1)^j \circ \kappa_2 \circ \gamma] \qquad (j = 0, \dots, k).$$

3.3. **The Weierstrass data.** We now take the Weierstrass data

$$G = c\frac{w}{z}, \qquad \eta = \frac{dz}{w} \qquad (c \in \boldsymbol{R}_+) \tag{3.8}$$

on M_k, where c is a positive real constant to be determined in (3.12). Define a holomorphic 2-differential Q

$$Q := \eta\, dG = \left(\frac{ck}{k+1}\right)\frac{z^2+1}{z^2(z^2-1)}\, dz^2. \tag{3.9}$$

(z,w)	$(0,0)$	(∞,∞)	$(1,0)$	$(-1,0)$	$(\pm i,*)$
$\operatorname{Ord} G$	$-k$	$-k$	k	k	0
$\operatorname{Ord}\eta$	$k-1$	$k-1$	0	0	0
$\operatorname{Ord} G\eta$	-1	-1	k	k	0
$\operatorname{Ord} G^2\eta$	$-(k+1)$	$-(k+1)$	$2k$	$2k$	0
$\operatorname{Ord} Q$	-2	-2	$k-1$	$k-1$	1

TABLE 1. Orders of G, η, $G\eta$, $G^2\eta$ and $Q = \eta\, dG$.

We call Q the *Hopf differential* because it will be the Hopf differential of the maxface when the construction is completed. The orders of G, η, $G\eta$, $G^2\eta$ and Q are listed as in Table 1, where $\operatorname{Ord}\omega = m$ (resp. $-m$) for a positive integer m if ω has a zero (resp. a pole) of order m. Then one can conclude that $\deg G = 2k$ for any $k \geq 1$.

Let

$$\hat{f}_{k,c} := \operatorname{Re}\int \Phi\colon \widetilde{M}_k \longrightarrow \boldsymbol{R}^3_1, \tag{3.10}$$

where Φ is the $\boldsymbol{C}^3$-valued 1-form as in (1.2) obtained by (G,η) in (3.8).

Lemma 3.2. *Suppose $\hat{f}_{k,c}$ as in* (3.10) *is well-defined on M_k. Then it is a complete maxface of genus k with 2 ends. Moreover, each end is asymptotic to the k-fold cover of the Lorentzian catenoid.*

Proof. Observe that η and $G^2\eta$ are holomorphic on M_k and have no common zeros, and $G^2\eta$ has poles of order $k+1$ at $(z,w) = (0,0)$ and (∞,∞). Thus the metric as in (1.1) gives a complete Riemannian metric on M_k. Hence $\hat{f}_{k,c}$ is a weakly complete maxface. Moreover, since G has poles at $(z,w) = (0,0)$ and (∞,∞), $|G| \neq 1$ at the ends. Then $\hat{f}_{k,c}$ is complete because of Fact 1.2. At each end, Q has a pole of order 2 and the ramification order of G is k. Then the Weierstrass representation (1.4) yields that the end is asymptotic to the k-fold cover of an end of the Lorentzian catenoid. □

Remark 3.3. The Hopf differential $Q(z)$ is real if $z \in \boldsymbol{R}$ or $z \in i\boldsymbol{R}$. Also, $Q(z)$ is pure imaginary if $|z| = 1$. Then the image of the real and imaginary axes on the z-plane are planar geodesics with respect to the first fundamental form of the surface, and the image of the unit circle consists of line segments joining singular points.

3.4. **The period problem.** In this section, we shall solve the period problem (1.3). The following lemma can be obtained by straightforward calculations:

Lemma 3.4. *Let Φ be as in* (1.2) *for the data* (3.8). *Then for automorphisms κ_j in* (3.6) *($j = 1,2$), it holds that*

$$\kappa_1^*\Phi^T = \begin{pmatrix} 1 & 0 & 0 \\ 0 & \cos 2k\lambda & -\sin 2k\lambda \\ 0 & \sin 2k\lambda & \cos 2k\lambda \end{pmatrix}\Phi^T, \quad \kappa_2^*\Phi^T = \begin{pmatrix} 1 & 0 & 0 \\ 0 & \cos k\lambda & \sin k\lambda \\ 0 & -\sin k\lambda & \cos k\lambda \end{pmatrix}\Phi^T,$$

where ^{T} stands for transposition.

Because of the matrices in Lemma 3.4, Lemma 3.1 implies that

Lemma 3.5. *The map $\hat{f}_{k,c}$ defined in* (3.10) *is single-valued on M_k if and only if the period condition* (1.3) *holds for the single loop γ in Figure 8.*

Now, we determine the value of $c \in \boldsymbol{R}_+$ in (3.8) such that the condition in Lemma 3.5 holds.

Since $G\eta = (c/z)dz$, it holds that

$$\operatorname{Re} \oint_\gamma G\eta = \operatorname{Re} \oint_\gamma c\, d\log z = \operatorname{Re}(2\pi i c) = 0.$$

So the condition (1.3) for γ is equivalent to

$$\oint_\gamma \eta + \overline{\oint_\gamma G^2\eta} = 0. \tag{3.11}$$

To calculate the integrals of the left-hand side, we take two paths on M_k as

$$\gamma_1 := \left\{ (z,w) = \left(t, e^{ki\lambda} \sqrt[k+1]{t(1-t^2)^k}\right) \;\middle|\; t : 1 \mapsto 0 \right\},$$
$$\gamma_2 := \left\{ (z,w) = \left(t, e^{-ki\lambda} \sqrt[k+1]{t(1-t^2)^k}\right) \;\middle|\; t : 0 \mapsto 1 \right\},$$

where we consider $\sqrt[k+1]{t(1-t^2)^k}$ as a positive real number. Roughly speaking, a closed loop $\gamma_1 * \gamma_2$ (the definition of $\gamma_1 * \gamma_2$ is given in the appendix) is homotopic to γ on $\overline{M}_k$. Here, γ_1 and γ_2 are parametrized regular curves on $\overline{M}_k$ from $t = 1$ to $t = 0$ and $t = 0$ to $t = 1$, respectively. Adding an exact form to $G^2\eta$, we have

$$G^2\eta + c^2 \frac{k+1}{k} d\left(\frac{w}{z}\right) = -2c^2 \frac{w}{1-z^2} dz.$$

Since the right-hand side does not have poles at $(z,w) = (0,0)$ and $(1,0)$, we have

$$\oint_\gamma G^2\eta = -2c^2 \oint_\gamma \frac{w}{1-z^2}\, dz = -2c^2 \left(\int_{\gamma_1} \frac{w}{1-z^2}\, dz + \int_{\gamma_2} \frac{w}{1-z^2}\, dz \right)$$
$$= -c^2 \cdot 4i \sin k\lambda \cdot A_k \qquad \left(A_k := \int_0^1 \sqrt[k+1]{\frac{t}{1-t^2}}\, dt \right).$$

On the other hand, since η does not have poles at $(z,w) = (0,0)$ and $(1,0)$, we have

$$\oint_\gamma \eta = \int_{\gamma_1} \eta + \int_{\gamma_2} \eta = 2i \sin k\lambda \cdot B_k \qquad \left(B_k := \int_0^1 \frac{dt}{\sqrt[k+1]{t(1-t^2)^k}} \right).$$

Therefore, if we set

$$c = c_k := \sqrt{\frac{B_k}{2A_k}} > 0, \tag{3.12}$$

then (3.11) holds for γ and hence

$$\hat{f}_k := \hat{f}_{k,c_k} \tag{3.13}$$

is single-valued on M_k. By Lemma 3.2, $\hat{f}_k$ is a complete maxface of genus k with 2 ends. See Figures 6, 9 and 10.

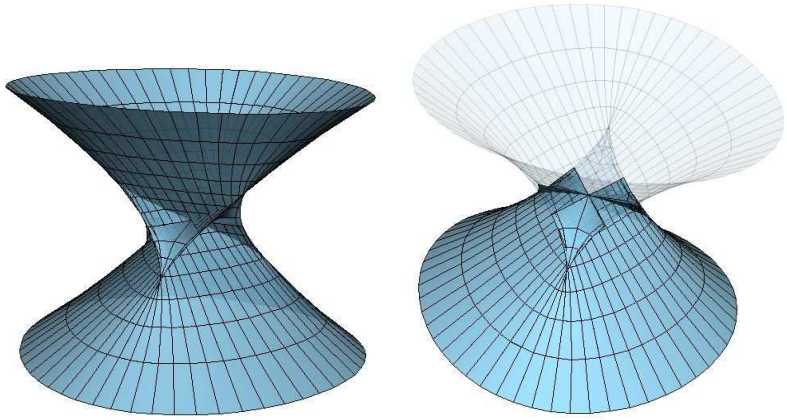

FIGURE 9. The example for $k = 2$ and half of it.

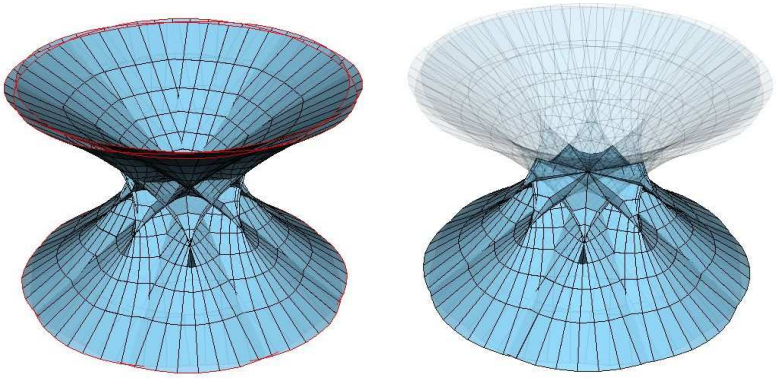

FIGURE 10. The example for $k = 3$ and half of it.

Now, we prove that $\hat{f}_1$ is embedded (in the wider sense, as in Definition II). When $k = 1$, each end is asymptotic to a Lorentzian catenoid, that is, each end has no self-intersection. Moreover, the x_0-component of $\hat{f}_1$ is calculated as

$$x_0 := -2\,\mathrm{Re}\int_o^p G\eta = -2c_1 \log|z| + \text{constant},$$

where $p = (z, w) \in M_1$. Hence $x_0 \to +\infty$ (resp. $-\infty$) when $(z, w) \to (0, 0)$ (resp. (∞, ∞)). This means that the two ends have no self-intersection outside a compact set in M_1. Hence $\hat{f}_1$ is embedded in the wider sense.

3.5. **Reduction for the even genus case.** When k is even, the Riemann surface $\overline{M}_k$ of genus $k = 2m$ is reduced to the Riemann surface

$$\overline{M}'_k = \left\{(Z, W) \in (\boldsymbol{C} \cup \{\infty\})^2\,;\, W^{2m+1} = Z^{m+1}\,(Z-1)^{2m}\right\}$$

of genus m, where m is a positive integer. As a submanifold of $(\boldsymbol{C} \cup \{\infty\})^2$, $\overline{M}'_k$ has singular points at $z = 0$, 1 and $z = \infty$. However, in a similar way to the case

of $\overline{M}_k$ (see (3.2)), the structure of a Riemann surface can be introduced to $\overline{M}_k'$. The map $\pi : \overline{M}_k' \ni (Z, W) \longmapsto Z \in \boldsymbol{C} \cup \{\infty\}$ is a meromorphic function of degree $2m+1$ with total branching number $6m$. Then, by the Riemann-Hurwitz relation, the genus of $\overline{M}_k'$ is equal to m. Let

$$M_k' = \overline{M}_k' \setminus \{(0,0), (\infty, \infty)\}. \tag{3.14}$$

Define a map ϖ_k from M_k of genus $k = 2m$ into M_k' of genus m as

$$\varpi_k : M_k \ni (z, w) \longmapsto (Z, W) = (z^2, zw) \in M_k'. \tag{3.15}$$

Then $\varpi_k(z, w) = \varpi_k(-z, -w)$ for any $(z, w) \in \overline{M}_k$ and hence ϖ_k is a double cover.

Let (G_1, η_1) be the Weierstrass data on M_k' given by

$$G_1 = c\frac{W}{Z}, \qquad \eta_1 = \frac{dZ}{2W},$$

which satisfy

$$G = \varpi_k^* G_1 = G_1 \circ \varpi_k, \qquad \eta = \varpi_k^* \eta_1.$$

The data (G_1, η_1) for $c = c_k$ as in (3.12) gives a maxface $f_k \colon M_k' \to \boldsymbol{R}_1^3$ such that $\hat{f}_k = f_k \circ \varpi_k$. Since $\deg G_1 = m$, all ends are embedded if and only if $m = 1$ (cf. [32, Theorem 4.11]). Moreover, if this is the case, embeddedness of f_2 can be shown in a similar way to the case of $\hat{f}_1$. Compare Figures 6 (for $k = 1$) and 9 for the case $k = 2$.

3.6. **Swallowtails and cuspidal cross caps of f_k.** In this section, we investigate the properties of the singular points.

Lemma 3.6. *The number c_k in* (3.12) *satisfies*

$$c_1 > 1 \qquad \textit{and} \qquad c_k > \frac{k^{\frac{1}{2(k+1)}}}{\sqrt{2}} \left(\frac{k}{k-1}\right)^{\frac{k-1}{2(k+1)}} \quad (k \geq 2).$$

In particular, for each $k = 1, 2, 3, \ldots$, it holds that

$$0 < \rho_k < 2 \qquad \left(\rho_k := c_k^{\frac{-2(k+1)}{k}}\right). \tag{3.16}$$

Proof. First, we consider the case $k \geq 2$. Set

$$V(s,t) := t(1-t^2)^k \left(\frac{1}{t(1-t^2)^k} - \frac{s^{k+1}t}{1-t^2}\right) = 1 - s^{k+1}t^2(1-t^2)^{k-1}$$

for $s \in \boldsymbol{R}$ and $t \in [0, 1]$. Then for each fixed value s, $V(s, t)$ attains a minimum at $t = 1/\sqrt{k}$, and

$$V\left(s, \frac{1}{\sqrt{k}}\right) = 1 - \frac{s^{k+1}}{k}\left(\frac{k-1}{k}\right)^{k-1}.$$

Hence if we set

$$s_k := k^{\frac{1}{k+1}} \left(\frac{k}{k-1}\right)^{\frac{k-1}{k+1}}, \tag{3.17}$$

then $V(s_k, t) \geq 0$ $(t \in [0, 1])$. Hence

$$\sqrt[k+1]{\frac{t}{1-t^2}} - s_k \frac{1}{\sqrt[k+1]{t(1-t^2)^k}} > 0$$

holds on $t \in [0,1]$, and then, we have

$$c_k = \sqrt{\frac{A_k}{2B_k}} > \sqrt{\frac{s_k}{2}} = \frac{1}{\sqrt{2}} k^{\frac{1}{2(k+1)}} \left(\frac{k}{k-1}\right)^{\frac{k-1}{2(k+1)}}.$$

This implies

$$0 < \rho_k < 2^{\frac{k+1}{k}} k^{-\frac{1}{k}} \left(\frac{k}{k-1}\right)^{\frac{1-k}{k}} = 2\left(\frac{2}{k}\right)^{\frac{1}{k}} \left(\frac{k-1}{k}\right)^{\frac{k-1}{k}} < 2.$$

Next, consider the case $k = 1$:

$$\begin{aligned} A_1 - 2B_1 &= \int_0^1 \left(\frac{1}{\sqrt{t(1-t^2)}} - 2\sqrt{\frac{t}{1-t^2}}\, dt \right) = \int_0^1 \left(\frac{1-2t}{\sqrt{t(1-t^2)}} \right) dt \\ &= \sqrt{2} \int_{-1}^2 \frac{u\, du}{\sqrt{(1-u^2)(3-u)}} \\ &= \sqrt{2} \left(\int_0^1 \frac{u\, du}{\sqrt{(1-u^2)(3-u)}} + \int_0^1 \frac{v\, dv}{\sqrt{(1-v^2)(3+v)}} \right) \\ &= \sqrt{2} \int_0^1 \frac{u}{\sqrt{1-u^2}} \left(\frac{1}{3-u} - \frac{1}{3+u} \right) du > 0, \end{aligned}$$

where we put $u = 1 - 2t$ and $v = -u$. Hence $c_1 = \sqrt{A_1/(2B_1)} > 1$, and then $\rho_1 < 1 < 2$. □

Lemma 3.7 (The singular curve)**.** *The set of singular points of $\hat{f}_k$ consists of* 2 *simple closed curves on M_k. The projection of the singular set onto the z-plane is shown in Figure 11.*

Proof. The set of singular points is represented as $\Sigma := \{p \in M_k\,;\, |G(p)| = 1\}$ (cf. Fact 1.1). Here, by (3.8), the condition $|G| = 1$ is equivalent to $|c_k w/z| = 1$, and then, by (3.1), it is equivalent to

$$\left| z - \frac{1}{z} \right|^2 = r^2 + \frac{1}{r^2} - 2\cos 2\theta = \rho_k \qquad \left(\rho_k = c_k^{\frac{-2(k+1)}{k}} \right),$$

where $z = re^{i\theta}$. Since $\rho_k \in (0,2)$ by Lemma 3.6, one can set

$$\Gamma_k := \arcsin \frac{\sqrt{\rho_k}}{2} \in \left(0, \frac{\pi}{4}\right).$$

Thus, the projection of the singular set onto the z-plane consists of two simple closed curves in the z-plane, contained in two angular domains:

$$\Delta_+ := \{-\Gamma_k < \arg z < \Gamma_k\}, \quad \text{and} \quad \Delta_- := \{\pi - \Gamma_k < \arg z < \pi + \Gamma_k\}.$$

We denote two subsets of the singular set Σ as

$$\Sigma_+ := \{p \in \Sigma\,;\, z(p) \in \Delta_+\}, \quad \text{and} \quad \Sigma_- := \{p \in \Sigma\,;\, z(p) \in \Delta_-\},$$

see Figure 11, where $z\colon M_k \ni (z,w) \mapsto z \in \boldsymbol{C}$ is the projection.

The loop $z(\Sigma_+)$ on the z-plane is surrounding the branch point $z = 1$ of the projection z. Then, the inverse image Σ_+ of this loop consists of $k+1$ copies of $z(\Sigma_+)$ which forms a single loop in M_k, that is, Σ_+ is a loop in M_k. Similarly so is Σ_-. □

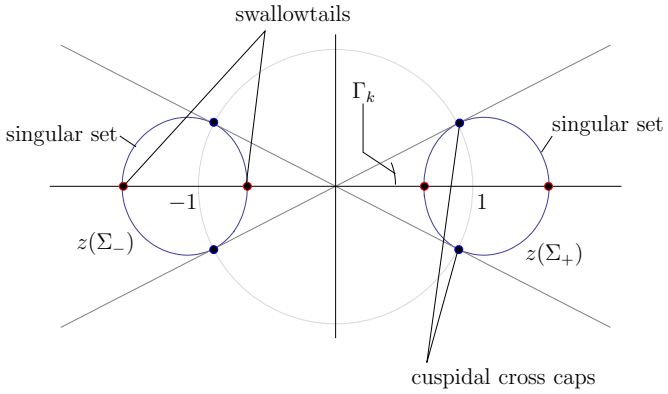

FIGURE 11. The singular set of $\hat{f}_k$.

Lemma 3.8. *On each connected component of the singular set in Lemma 3.7, there are $2(k+1)$ swallowtails and $2(k+1)$ cuspidal cross caps. Singular points other than these points are cuspidal edges.*

Proof. Let α and β be as in (1.6):

$$\alpha := \frac{dG}{G^2\eta} = \frac{Q}{(G\eta)^2} = \frac{z^2+1}{z^2-1} = 1 - \frac{2}{z^2-1}, \qquad \beta := \left(\frac{G}{dG}d\alpha\right) = z^2 - \frac{1}{z^2}.$$

Then

$$2\operatorname{Re}\alpha = \frac{z^2+1}{z^2-1} + \frac{\bar{z}^2+1}{\bar{z}^2-1} = 2\frac{|z|^4-1}{|z^2-1|^2} = 0 \qquad \text{if and only if} \qquad |z| = 1,$$

and $\operatorname{Im}\alpha = 0$ if and only if $z \in \boldsymbol{R} \cup i\boldsymbol{R}$. On the other hand, since $\operatorname{Re}\beta = \left(r^2 - r^{-2}\right)\cos 2\theta$ $(z = re^{i\theta})$,

$$\operatorname{Re}\beta = 0 \qquad \text{if and only if} \qquad |z| = 1 \quad \text{or} \quad \arg z = \frac{\pi}{4}, \frac{3\pi}{4}, \frac{5\pi}{4}, \frac{7\pi}{4}.$$

Finally, since $\operatorname{Im}\beta = \left(r^2 + r^{-2}\right)\sin 2\theta$, $\operatorname{Im}\beta = 0$ if and only if $z \in \boldsymbol{R} \cup i\boldsymbol{R}$.

Then by Fact 1.3, there are two swallowtails and two cuspidal cross caps on Σ_+, on the z-plane. Since M_k is a $(k+1)$-fold branched cover of the z-plane, we have the conclusion. □

When $k = 2m$ is even, both $\hat{f}_m$ and f_k give maxfaces of genus m with 2 ends. Moreover, each end is asymptotic to the m-fold cover of the Lorentzian (elliptic) catenoid.

Corollary 3.9. *When $k = 2m$, $\hat{f}_m$ and f_k are not congruent.*

Proof. The number of swallowtails on the image of $\hat{f}_m$ is $4m+4$. On the other hand, the number of swallowtails on the image of f_k $(k = 2m)$ is $4m+2$, which proves the assertion. □

4. Proof of the second part of Theorem B

In this section, we shall deform the maxfaces given in the previous section to CMC-1 faces in de Sitter space. The technique we use here is similar to that in

[27]. However, we need much more technical arguments because the maxfaces f_k in the previous section do not have *non-degenerate period problem* as in [27, Section 5]. So, we accomplish the deformation by computing the derivative of the period matrices.

4.1. **Preliminaries.** First, we recall some fundamental facts about CMC-1 faces in de Sitter space. For detailed expressions, see [8, 9], or [12]. Let $\boldsymbol{R}^4_1$ be the Minkowski 4-space with the metric $\langle\ ,\ \rangle$ of signature $(-,+,+,+)$. Then de Sitter 3-space is expressed as

$$S^3_1 = \{X \in \boldsymbol{R}^4_1 ;\, \langle X, X\rangle = 1\}$$

with metric induced from $\boldsymbol{R}^4_1$, which is a simply-connected Lorentzian 3-manifold with constant sectional curvature 1. We identify $\boldsymbol{R}^4_1$ with the set of 2×2 Hermitian matrices $\mathrm{Herm}(2)$ by

$$\boldsymbol{R}^4_1 \ni (x_0, x_1, x_2, x_3) \leftrightarrow \begin{pmatrix} x_0 + x_3 & x_1 + ix_2 \\ x_1 - ix_2 & x_0 - x_3 \end{pmatrix} \in \mathrm{Herm}(2). \tag{4.1}$$

Then de Sitter 3-space is represented as

$$\begin{aligned} S^3_1 &= \{X \in \mathrm{Herm}(2) \,;\, \det X = -1\} \\ &= \{Fe_3F^* \,;\, F \in \mathrm{SL}_2\boldsymbol{C}\} = \mathrm{SL}_2\boldsymbol{C}/\,\mathrm{SU}_{1,1} \qquad \left(e_3 := \begin{pmatrix} 1 & 0 \\ 0 & -1 \end{pmatrix}\right). \end{aligned}$$

The first author [8] introduced the notion of CMC-1 faces in S^3_1, which corresponds to maxfaces in $\boldsymbol{R}^3_1$.

To state the Weierstrass-type representation formula, we prepare some notions:

Definition 4.1. A pair (G, Q) of a meromorphic function G and a holomorphic 2-differential Q on M is said to be *admissible* if

$$ds^2_{\#} = \left(1 + |G|^2\right)^2 \left|\frac{Q}{dG}\right|^2 \tag{4.2}$$

is a (positive definite) Riemannian metric on M.

Proposition 4.2. *Let M be a Riemann surface and (G, Q) an admissible pair on M. Let $F = (F_{ij})\colon \widetilde{M} \to \mathrm{SL}_2\boldsymbol{C}$ be a holomorphic map of the universal cover $\widetilde{M}$ of M such that*

$$dF\, F^{-1} = \Psi \qquad \left(\Psi := \begin{pmatrix} G & -G^2 \\ 1 & -G \end{pmatrix} \frac{Q}{dG}\right). \tag{4.3}$$

Then F is a null holomorphic immersion, that is, F is a holomorphic immersion such that $\det(dF/dz)$ vanishes identically for each local complex coordinate z on M. And

$$f := Fe_3F^*\colon \widetilde{M} \longrightarrow S^3_1 \tag{4.4}$$

is a CMC-1 face if $|g|$ is not identically 1, where g is a meromorphic function on $\widetilde{M}$ defined by

$$g := -\frac{dF_{12}}{dF_{11}} = -\frac{dF_{22}}{dF_{21}}. \tag{4.5}$$

The induced metric ds^2 *and the second fundamental form* $\mathrm{I\!I}$ *are expressed as*

$$ds^2 = (1-|g|^2)^2 \left|\frac{Q}{dg}\right|^2, \qquad \mathrm{I\!I} = Q + \overline{Q} + ds^2, \tag{4.6}$$

*respectively. Conversely, any CMC-*1 *face is obtained in this manner.*

Remark 4.3. (1) The equation (4.3) should be regarded as an equation on the universal cover $\widetilde{M}$ (see (A.6) in the appendix). However, for simplicity, we use the notation here.

(2) The condition that $|g|$ is not identical to 1 is necessary to avoid the example all of whose points are singular points. Such an example is unique up to isometry, whose image is a lightlike line in S^3_1 (see [12, Remark 1.3]).

Proof of Proposition 4.2. Though the statement of this proposition is mentioned in [8, Theorem 1.2], the proof is not given there. So we give a proof here. By (4.3), F is a null holomorphic map from $\widetilde{M}$ into $\mathrm{SL}_2\boldsymbol{C}$, and admissibility implies that F is an immersion. Moreover, if $|g|$ is not identically 1, $\det[Fe_3F^*]$ does not vanish identically. Hence by Proposition 4.7 in [8], $f = Fe_eF^*$ is a CMC-1 face. □

The meromorphic function G, the holomorphic 2-differential Q and the (multi-valued) meromorphic function g in Proposition 4.2 are called the *hyperbolic Gauss map*, the *Hopf differential*, and the *secondary Gauss map*, respectively. We call F the *holomorphic null lift* of the CMC-1 face f. These holomorphic data are related by

$$S(g) - S(G) = 2Q, \qquad \left(S(h) := \left[\left(\frac{h''}{h'}\right)' - \frac{1}{2}\left(\frac{h''}{h'}\right)^2\right] dz^2,\ ' = \frac{d}{dz}\right), \tag{4.7}$$

where z is a local complex coordinate on M and $S(\cdot)$ is the Schwarzian derivative.

For an admissible pair (G, Q) on M, there exists a representation $\rho_F\colon \pi_1(M) \to \mathrm{SL}_2\boldsymbol{C}$ associated with the solution F of (4.3) as in Proposition A.4 in the appendix:

$$F \circ \tau = F\rho_F(\tau)^{-1} \qquad \big(\tau \in \pi_1(M)\big), \tag{4.8}$$

where $\tau \in \pi_1(M)$ is considered as a covering transformation of the universal cover $\widetilde{M}$, as in (A.2).

To deform maxfaces to CMC-1 faces, the following facts, which are proved in [27] for CMC-1 surfaces in H^3, play important roles:

Lemma 4.4 (cf. [27, Lemma 4.8])**.** *Take an admissible pair* (G, Q) *on a Riemann surface* M*. Then* $(G, Q_t = tQ)$ *is also an admissible pair for all* $t \in \boldsymbol{R} \setminus \{0\}$*. Let* $F := F_t\colon \widetilde{M} \to \mathrm{SL}_2\boldsymbol{C}$ *be a solution of*

$$dFF^{-1} = t\Psi_0, \qquad \Psi_0 = \begin{pmatrix} G & -G^2 \\ 1 & -G \end{pmatrix} \frac{Q}{dG}, \tag{4.9}$$

with the initial condition $F_t(o) = \iota(t)$*, where* $\iota(t)$ *is a smooth* $\mathrm{SL}_2\boldsymbol{C}$*-valued function in* t *with* $\iota(0) = e_0$*, where*

$$e_0 := \begin{pmatrix} 1 & 0 \\ 0 & 1 \end{pmatrix} \tag{4.10}$$

is the identity matrix and $o \in \widetilde{M}$ *is a base point. Let* $\rho_t = \rho_{F_t}(\tau)$ *for* $\tau \in \pi_1(M)$*, where* ρ_{F_t} *is a representation as in* (4.8)*. Then it holds that*

$$\left.\frac{d}{dt}\right|_{t=0} (\rho_t)^{-1} = \int_\gamma \Psi_0, \tag{4.11}$$

and γ *is a loop in* M *which represents* τ*.*

Proof. By (4.9), F_0 is a constant map. Differentiating (4.9), we have $d\dot{F} = \Psi_0 \iota(0)$, where $\dot{F} = (\partial/\partial t)|_{t=0} F_t$. Hence we have

$$\left.\frac{d}{dt}\right|_{t=0} \oint_\gamma dF_t = \oint_\gamma \Psi_0.$$

Here, the left-hand side is computed as

$$\left.\frac{d}{dt}\right|_{t=0} \Big(F_t(o)(\rho_t)^{-1} - F_t(o) \Big) = \left.\frac{d}{dt}\right|_{t=0} \Big(\iota(t)(\rho_t)^{-1} - \iota(t) \Big) = \left.\frac{d}{dt}\right|_{t=0} (\rho_t)^{-1},$$

because $\iota(0) = e_0$. Hence we have the conclusion. □

Similar to Definition I in the introduction, we define completeness and weak completeness of CMC-1 faces:

Definition 4.5 ([12, Definitions 1.2 and 1.3]). A CMC-1 face $f\colon M \to S^3_1$ is called *complete* if there exists a symmetric 2-tensor T which vanishes outside a compact set in M, such that $ds^2 + T$ is a complete Riemannian metric on M, where ds^2 is the induced metric by f as in (4.6). On the other hand, f is called *weakly complete* if the metric $ds^2_\#$ in (4.2) is complete.

Like as in the case of maxfaces, we have

Fact 4.6 ([33])**.** *Let* M *be a Riemann surface, and* $f\colon M \to S^3_1$ *a weakly complete CMC-1 face. Then* f *is complete if and only if there exists a compact Riemann surface* $\overline{M}$ *and a finite number of points* $p_1, \ldots, p_n \in \overline{M}$ *such that* M *is conformally equivalent to* $\overline{M} \setminus \{p_1, \ldots, p_n\}$*, and the set of singular points* $\Sigma = \{p \in M\,;\, |g(p)| = 1\}$ *is compact.*

4.2. **The holomorphic data.** Let k be a positive integer, and take the Riemann surface M_k as in (3.3). Take a meromorphic function G, a holomorphic 1-form η and a holomorphic 2-differential Q_t ($t \in \boldsymbol{R}$) on M_k as

$$G := c_k \frac{w}{z}, \qquad Q_t := \frac{t}{c_k} Q \left(= \frac{tk}{k+1} \frac{z^2+1}{z^2(z^2-1)} dz^2 \right), \tag{4.12}$$

where (G, η) are the Weierstrass data as in (3.8), $Q = \eta dG$ is as in (3.9), and $c = c_k$ is as in (3.12). We set

$$\Psi := t\Psi_0, \qquad \Psi_0 := \frac{1}{c_k} \begin{pmatrix} G & -G^2 \\ 1 & -G \end{pmatrix} \frac{Q}{dG}. \tag{4.13}$$

Then one can easily show that (G, Q) (and then (G, Q_t) for $t \neq 0$) is an admissible pair on M_k, and the metric (4.2) is complete.

Then the second part of Theorem B is a conclusion of the following

Proposition 4.7. *For each positive integer* $k = 1, 2, 3 \ldots$*, there exists a positive number* $\varepsilon = \varepsilon(k)$ *such that for each real number* t *with* $0 < |t| < \varepsilon$*, there exists a complete CMC-1 face* $\hat{f}_{k,t}\colon M_k \to S^3_1$ *whose hyperbolic Gauss map* G *and Hopf differential* Q_t *are given as in* (4.12)*.*

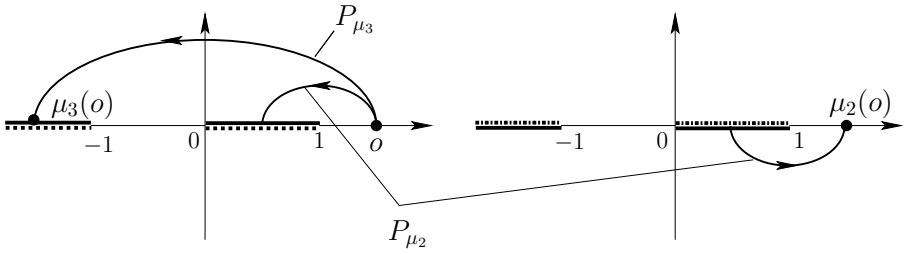

FIGURE 12. Paths P_{μ_1}, P_{μ_2} and P_{μ_3} (P_{μ_1} is the constant path at o).

Remark 4.8. Consider $\hat{f}_{k,t}$ as a map into the Minkowski space $\boldsymbol{R}^4_1$, and let

$$\tilde{f}_{k,t} = \frac{1}{t}\hat{f}_{k,t}\colon M_k \longrightarrow S^3_1(t^2) = \left\{ X \in \boldsymbol{R}^4_1;\, \langle X, X\rangle = \frac{1}{t^2} \right\} \subset \boldsymbol{R}^4_1,$$

where $S^3_1(t^2)$ is de Sitter 3-space of constant sectional curvature t^2. Then $\tilde{f}_{k,t}$ is a surface of mean curvature t in $S^3_1(t^2)$. Then taking the limit as $t \to 0$ in a similar way as in [30], $\tilde{f}_{k,t}$ converges to the maxface $\hat{f}_k$ as in the previous section. In this sense, the method provided here is considered as a "deformation".

4.3. **Representation of reflections.** The proof is done by a (refined version of) the reflection method, which was introduced in [27] for CMC-1 surfaces in the hyperbolic space. To do this, we first take the reflections on the universal cover $\widetilde{M}_k$ of M_k.

Let μ_j ($j = 1, 2, 3$) be the reflections on M_k as in (3.5). For a matrix $a = (a_{ij})_{i,j=1,2} \in \mathrm{SL}_2\boldsymbol{C}$ and a holomorphic function h on a Riemann surface M, we set

$$a \star h := \frac{a_{11}h + a_{12}}{a_{21}h + a_{22}}. \tag{4.14}$$

The following lemma is a direct conclusion of (3.5):

Lemma 4.9. *The pair (G, Q_t) as in* (4.12) *satisfies*

$$\overline{G \circ \mu_j} = \sigma_j \star G, \qquad \overline{Q_t \circ \mu_j} = Q_t \qquad (j = 1, 2, 3),$$

where

$$\sigma_1 = \begin{pmatrix} 1 & 0 \\ 0 & 1 \end{pmatrix} (= e_0), \quad \sigma_2 = \begin{pmatrix} \psi^{-2} & 0 \\ 0 & \psi^2 \end{pmatrix}, \quad \sigma_3 = \begin{pmatrix} \psi^{-1} & 0 \\ 0 & \psi \end{pmatrix}, \tag{4.15}$$

and

$$\psi := e^{ki\lambda/2} = \exp\left(\frac{i\pi k}{2(k+1)}\right) \qquad \left(\lambda = \frac{\pi}{k+1}\right). \tag{4.16}$$

Namely, (G, Q_t) is μ_j-invariant ($j = 1, 2, 3$) in the sense of (A.9) *in the appendix.*

We remark that we do not use μ_4 here, because (G, Q) is not μ_4-invariant in the sense of (A.9) as in the appendix. In fact, $\overline{Q \circ \mu_4} = -Q$ holds.

We fix the base point $o \in M_k$ as in (3.7) and take paths P_{μ_j} on M_k associated to μ_j as in the appendix which join o and $\mu_j(o)$ as in Figure 12 for each $j = 1, 2, 3$. (In Figure 12, the left-hand z-plane is the sheet containing o and the right-hand z-plane is the sheet containing $\mu_2(o)$. These two sheets are connected along two intervals $(0, 1)$ and $(-\infty, -1)$ on each real axis.)

Here P_{μ_1} is the constant path at o. Then one can take the lift $\tilde{\mu}_j$ $(j = 1, 2, 3)$ (as orientation-reversing involutions on $\widetilde{M}_k$) of $\mu_j : M_k \to M_k$ with respect to the path P_{μ_j}, see (A.4) in the appendix.

Then by Proposition A.2, we have

Lemma 4.10. *Let γ be the loop as in Figure 8, and let κ_j $(j = 1, 2)$ be the automorphisms of M_k as in* (3.6)*. Then*

$$[\gamma] = \tilde{\mu}_3 \circ \tilde{\mu}_2 \circ \tilde{\mu}_3 \circ \tilde{\mu}_1,$$
$$[\kappa_2 \circ \gamma] = \tilde{\mu}_3 \circ \tilde{\mu}_1 \circ \tilde{\mu}_3 \circ \tilde{\mu}_2,$$
$$[(\kappa_1)^j \circ \gamma] = (\tilde{\mu}_2 \circ \tilde{\mu}_1)^j \circ [\gamma] \circ (\tilde{\mu}_1 \circ \tilde{\mu}_2)^j,$$
$$[(\kappa_1)^j \circ \kappa_2 \circ \gamma] = (\tilde{\mu}_2 \circ \tilde{\mu}_1)^j \circ [\kappa_2 \circ \gamma] \circ (\tilde{\mu}_1 \circ \tilde{\mu}_2)^j$$

hold, where [ ] denotes the homotopy class and the meaning of the above equalities is explained in Remark A.3. On the other hand, let τ_0 and τ_∞ be covering transformations corresponding to counterclockwise simple closed loops γ_0 and γ_∞ in M_k around $(z, w) = (0, 0)$ and (∞, ∞), respectively. (The projections of γ_0 and γ_∞ to the z-plane are both $(k+1)$-fold coverings of simple closed loops in $\boldsymbol{C}$.)

Then

$$\tau_0 = (\tilde{\mu}_3 \circ \tilde{\mu}_2)^{2(k+1)}, \qquad \tau_\infty = (\tilde{\mu}_1 \circ \tilde{\mu}_3)^{2(k+1)}$$

hold. Namely, $\{\tilde{\mu}_1, \tilde{\mu}_2, \tilde{\mu}_3\}$ is a generator of the fundamental group of M_k in the sense of Definition A.7 in the appendix.

For each $t \in \boldsymbol{R}$ and $b \in \mathrm{SL}_2 \boldsymbol{C}$, denote by

$$F = F_{t,b} \colon \widetilde{M}_k \longrightarrow \mathrm{SL}_2 \boldsymbol{C}$$

the unique solution of the differential equation

$$dFF^{-1} = \Psi = t\Psi_0, \qquad F(o) = b, \tag{4.17}$$

where Ψ_0 is as in (4.13). Then by Lemma 4.9 and Theorem A.6 in the appendix, there exists $\tilde{\rho}_{j,t,b} \in \mathrm{SL}_2 \boldsymbol{C}$ such that

$$\overline{F_{t,b} \circ \tilde{\mu}_j} = \sigma_j F_{t,b}(\tilde{\rho}_{j,t,b})^{-1} \qquad (j = 1, 2, 3), \tag{4.18}$$

where σ_j $(j = 1, 2, 3)$ are the matrices given in (4.15). By Proposition A.9, the group generated by $\{\tilde{\rho}_{j,t,b}\}_{j=1,2,3}$ contains the subgroup $\rho_F(\pi_1(M_k))$ given in (4.8).

Then we have the following by Lemma 4.10 and Theorem A.10, which is the key to our construction:

Proposition 4.11. *If $\tilde{\rho}_{j,t,b} \in \mathrm{SU}_{1,1}$ for $j = 1, 2, 3$, then the CMC-1 face*

$$\hat{f}_{t,b} := (F_{t,b}) e_3 (F_{t,b})^*$$

corresponding to $F_{t,b}$ as in (4.4) *is well-defined on M_k.*

Here, we summarize properties of the matrices $\tilde{\rho}_{j,t,b}$:

Proposition 4.12. *Suppose a, $b \in \mathrm{SL}_2 \boldsymbol{C}$. Then the following hold*:

(1) $\tilde{\rho}_{j,t,ba} = \bar{a}^{-1}(\tilde{\rho}_{j,t,b})a$.
(2) $\tilde{\rho}_{j,0,b} = \bar{b}^{-1}(\sigma_j)b$. *In particular,* $\tilde{\rho}_{j,0,e_0} = \sigma_j$.

Proof. Since $F_{t,ba} = (F_{t,b})a$, (1) holds. When $t = 0$, $F_{0,b} = b$. Then

$$\bar{b} = \overline{F_{0,b}} = \overline{F_{0,b} \circ \tilde{\mu}_j} = \sigma_j F_{0,b}(\rho_j)^{-1} = \sigma_j b(\rho_j)^{-1},$$

where $\rho_j = \tilde{\rho}_{j,0,b}$, which implies (2). □

4.4. **Existence of $\hat{f}_k$.** The existence part of Proposition 4.7 is a straightforward conclusion of the following proposition, because of Proposition 4.11:

Proposition 4.13. *For a sufficiently small positive number ε, there exists a real analytic family $\iota(t)$ of matrices in $\mathrm{SL}_2\boldsymbol{C}$ such that $\tilde{\rho}_{j,t,\iota(t)} \in \mathrm{SU}_{1,1}$ $(j = 1, 2, 3)$ holds if $0 < |t| < \varepsilon$.*

The proof is divided into three steps (Claims 1–3):

Claim 1. *For $t \in \boldsymbol{R}$ and for any real matrix $b \in \mathrm{SL}_2\boldsymbol{R}$, it holds that $\tilde{\rho}_{1,t,b} = e_0$.*

In fact, substituting o into (4.18) for $j = 1$, we have Claim 1.

Claim 2. *For sufficiently small $\varepsilon > 0$, there exists a real analytic family $\{\iota(t)\,;\, |t| < \varepsilon\}$ of matrices in $\mathrm{SL}_2\boldsymbol{R}$ such that $\iota(0) = e_0$ and $\tilde{\rho}_{2,t,\iota(t)} = \sigma_2$.*

Proof. Since $(\mu_2 \circ \mu_1)^{k+1} = \mathrm{id}_{M_k}$ holds, where id_{M_k} is the identity map on M_k, then by Proposition A.2 in the appendix, $(\tilde{\mu}_2 \circ \tilde{\mu}_1)^{k+1}$ is a covering transformation on $\widetilde{M_k}$. In fact, such a covering transformation corresponds to the counterclockwise simple closed loop on M_k surrounding $(z, w) = (1, 0)$, i.e., $(\tilde{\mu}_2 \circ \tilde{\mu}_1)^{k+1} = \mathrm{id}_{\widetilde{M_k}}$. Then by Proposition A.9,

$$e_0 = \rho_F(\mathrm{id}_{\widetilde{M_k}}) = \big(\overline{\sigma_2}\sigma_1\big)^{k+1}\big(\overline{\rho_2}\rho_1\big)^{k+1} = (-1)^k\big(\overline{\rho_2}\rho_1\big)^{k+1},$$

where $\rho_j = \tilde{\rho}_{j,t,e_0}$. Hence we have

$$(\rho_2)^{k+1} = (-1)^k e_0. \tag{4.19}$$

Since $\tilde{\rho}_{2,t,e_0}$ tends to $\tilde{\rho}_{2,0,e_0} = \sigma_2$ as $t \to 0$ (see (2) of Proposition 4.12), the equality (4.19) implies that the eigenvalues of $\tilde{\rho}_{2,t,e_0}$ are $\{\psi^{\pm 2}\}$, where ψ is given in (4.16). Hence

$$\operatorname{trace}\tilde{\rho}_{2,t,e_0} = 2\cos(k\lambda) \qquad \left(\lambda = \frac{\pi}{k+1}\right).$$

Then by (A.12), one can write

$$\tilde{\rho}_{2,t,e_0} = \begin{pmatrix} \cos(k\lambda) - iu(t) & is_1(t) \\ is_2(t) & \cos(k\lambda) + iu(t) \end{pmatrix} \qquad \big((\cos k\lambda)^2 + u(t)^2 + s_1(t)s_2(t) = 1\big),$$

where $u = u(t)$, $s_j = s_j(t)$ $(j = 1, 2)$ are real analytic functions in t. Since $\tilde{\rho}_{2,0,e_0} = \sigma_2$, we have that

$$u(0) = \sin(k\lambda), \qquad s_1(0) = s_2(0) = 0. \tag{4.20}$$

Let

$$\iota(t) := \frac{1}{\sqrt{2\big((\sin k\lambda)^2 + u(t)\sin(k\lambda)\big)}} \begin{pmatrix} u(t) + \sin(k\lambda) & s_1(t) \\ -s_2(t) & u(t) + \sin(k\lambda) \end{pmatrix}.$$

By (4.20), $(\sin k\lambda)^2 + u(t)\sin(k\lambda) > 0$ for sufficient small t, and hence $\iota(t)$ is a real matrix. It can be easily checked that $\iota(t)^{-1}\tilde{\rho}_{2,t,e_0}\iota(t) = \sigma_2$. Then (1) of Proposition 4.12 yields the assertion. □

Claim 3. *For $\iota(t)$ in Claim 2, it holds that*

$$\tilde{\rho}_{3,t,\iota(t)} = \begin{pmatrix} q(t) & ir_1(t) \\ ir_2(t) & \overline{q(t)} \end{pmatrix} \qquad (|q(t)|^2 + r_1(t)r_2(t) = 1), \tag{4.21}$$

where $q(t)$ is a complex-valued real-analytic function and $r_j(t)$ $(j = 1, 2)$ are real-valued real-analytic functions in t such that

$$q(0) = \psi^{-1}, \qquad r_1(0) = r_2(0) = 0. \tag{4.22}$$

Moreover, for $t \neq 0$ with sufficiently small absolute value,

$$r_1(t)r_2(t) < 0 \qquad \text{or equivalently,} \quad |q(t)| > 1 \tag{4.23}$$

holds.

The inequality (4.23) corresponds to the argument in [27, Lemma 6.10]. If (4.23) holds, we can prove the existence of the desired deformation $F_{t,\iota_1(t)}$ by modifying $\iota(t)$ by $\iota_1(t)$, as we shall see later. If $r_1(0)r_2(0)$ had been negative, Claim 3 would be obvious. However, in our case, (4.22) implies $r_1(0)r_2(0) = 0$, although all of the examples in [27] satisfy $r_1(0)r_2(0) \neq 0$. We show (4.23) by examining the derivative of the monodromy matrix. Set

$$F_t := F_{t,\iota(t)}, \tag{4.24}$$

$$\rho_j = \tilde{\rho}_{j,t,\iota(t)} \qquad (j = 1, 2, 3). \tag{4.25}$$

Then by Claims 1 and 2, we have

$$\rho_1 = e_0, \qquad \rho_2 = \sigma_2. \tag{4.26}$$

Moreover, by Theorem A.6, ρ_3 is written as in (4.21), and by (2) in Proposition 4.12 and the fact that $\iota(0) = e_0$, we have $\rho_3 \to \sigma_3$ as $t \to 0$. Hence q, r_1 and r_2 in (4.21) satisfy (4.22).

Let τ_0 and τ_∞ be the covering transformations on $\widetilde{M}_k$ given in Lemma 4.10. Since the initial value $\iota(t) = F_t(o)$ is real analytic in t, so are $\rho_{F_t}(\tau_0)$ and $\rho_{F_t}(\tau_\infty)$.

Lemma 4.14. *$F_t := F_{t,\iota(t)}$ satisfies*

$$\operatorname{trace} \rho_{F_t}(\tau_0) = (-1)^k 2\cos(\pi\nu_0), \quad \operatorname{trace} \rho_{F_t}(\tau_\infty) = (-1)^k 2\cos(\pi\nu_\infty), \tag{4.27}$$

where

$$\nu_0 = \nu_0(t) := k\sqrt{1 + 4t\frac{k+1}{k}}, \tag{4.28}$$

$$\nu_\infty = \nu_\infty(t) := k\sqrt{1 - 4t\frac{k+1}{k}}. \tag{4.29}$$

Proof. Let g be the secondary Gauss map of F_t. Setting $z = \zeta^{k+1}$, we can take a complex coordinate ζ around $(0, 0)$. Since G is a meromorphic function and Q_t has a pole of order 2 at $(0, 0)$, (4.7) implies that the Schwarzian derivative $S(g)$ has a pole of order 2 at $(0, 0)$. Hence there exist $a \in \mathrm{SL}_2 \boldsymbol{C}$ and a constant ν_0 such that

$$a \star g = \zeta^{\nu_0}\big(1 + o(1)\big), \tag{4.30}$$

where $o(\cdot)$ denotes a higher order term. Here, since G has a pole of order k at $(0, 0)$, and

$$Q_t = \frac{tk}{k+1}\frac{z^2+1}{z^2(z^2-1)}dz^2 = -\frac{tk(k+1)}{\zeta^2}\big(1 + o(1)\big)d\zeta^2$$

(4.7) implies that (see [31, page 233])

$$S(g) = S(G) + 2Q_t = \frac{1}{2\zeta^2}\Big((1-k^2) - 4tk(k+1) + o(1)\Big)d\zeta^2.$$

Similarly, (4.30) implies that

$$S(g) = \frac{1}{2\zeta^2}(1-\nu_0^2)d\zeta^2.$$

Thus, ν_0 coincides with (4.28). Note that ν_0 is a real number for t with sufficiently small absolute value.

Comparing the relation $g\circ\tau_0 = \rho_{F_t}(\tau_0)\star g$ with (4.30), we can conclude that the eigenvalues of $\rho_{F_t}(\tau_0)$ are equal to those of the monodromy matrix of the function $\zeta \mapsto \zeta^{\nu_0}$ up to sign. Then the eigenvalues of $\rho_{F_t}(\tau_0)$ are

$$\{e^{i\pi\nu_0}, e^{-i\pi\nu_0}\} \quad \text{or} \quad \{-e^{i\pi\nu_0}, -e^{-i\pi\nu_0}\}. \tag{4.31}$$

Similarly, setting $1/z = \zeta^{k+1}$, we take a complex coordinate ζ around (∞,∞). Then we have (4.29), and the eigenvalues of $\rho_{F_t}(\tau_\infty)$ are

$$\{e^{i\pi\nu_\infty}, e^{-i\pi\nu_\infty}\} \quad \text{or} \quad \{-e^{i\pi\nu_\infty}, -e^{-i\pi\nu_\infty}\}. \tag{4.32}$$

On the other hand, by Lemma 4.10 and Proposition A.9 in the appendix, we have

$$\rho_{F_t}(\tau_0) = \left[\left(\overline{\sigma_3}\sigma_2\right)^{2(k+1)}\right]\left(\overline{\rho_3}\rho_2\right)^{2(k+1)} = (-1)^k\left(\overline{\rho_3}\rho_2\right)^{2(k+1)}, \tag{4.33}$$

$$\rho_{F_t}(\tau_\infty) = (-1)^k\left(\overline{\rho_1}\rho_3\right)^{2(k+1)}. \tag{4.34}$$

Here, by (2) in Proposition 4.12 and Claim 2, $\rho_j \to \sigma_j$ $(t\to 0)$ holds for $j = 1,2,3$. Since σ_j $(j=1,2,3)$ are given explicitly in (4.15), we have that, as $t\to 0$,

$$\rho_{F_t}(\tau_0) \to (-1)^k\left(\sigma_2\overline{\sigma_3}\right)^{2(k+1)} = (-1)^{2k}e_0 = e_0, \quad \text{and} \quad \rho_{F_t}(\tau_\infty)\to e_0. \tag{4.35}$$

Then the eigenvalues of $\rho_{F_t}(\tau_0)$ and $\rho_{F_t}(\tau_\infty)$ tend to 1 as $t\to 0$. Hence by real analyticity, the right-hand possibilities for eigenvalues in (4.31) and (4.32) never occur, which implies the conclusion. □

Lemma 4.15. *$F_t := F_{t,\iota(t)}$ satisfies*

$$\left.\frac{d}{dt}\right|_{t=0}\rho_{F_t}(\tau_0)^{-1} = 2(k+1)\pi i\begin{pmatrix}1 & 0\\ 0 & -1\end{pmatrix},$$
$$\left.\frac{d}{dt}\right|_{t=0}\rho_{F_t}(\tau_\infty)^{-1} = -2(k+1)\pi i\begin{pmatrix}1 & 0\\ 0 & -1\end{pmatrix}.$$

Proof. As in the proof of the previous lemma, we can take the complex coordinate ζ around $(0,0)$ such that $z = \zeta^{k+1}$. Then G and Q are expressed in terms of ζ, and by (4.11) and (4.13), we have

$$\begin{aligned}\left.\frac{d}{dt}\right|_{t=0}\rho_{F_t}(\tau_0)^{-1} &= \oint_{\gamma_0}\frac{1}{c_k}\begin{pmatrix}G & -G^2\\ 1 & -G\end{pmatrix}\frac{Q}{dG}\\ &= 2\pi i\operatorname*{Res}_{\zeta=0}\frac{1}{c_k}\begin{pmatrix}G & -G^2\\ 1 & -G\end{pmatrix}\frac{Q}{dG} = 2\pi i\begin{pmatrix}k+1 & 0\\ 0 & -(k+1)\end{pmatrix},\end{aligned}$$

where γ_0 is the loop surrounding $(0,0)$ given in Lemma 4.10. Hence we have the conclusion for $\rho_{F_t}(\tau_0)$. The derivative of $\rho_{F_t}(\tau_\infty)$ is obtained in a similar way. □

Now, we shall prove Claim 3:

Proof of Claim 3. We have already shown (4.21) and (4.22). Then it is sufficient to show that $|q(t)| > 1$ for $t \neq 0$ with sufficiently small $|t|$. We set $a_0(t) = \overline{\rho_3}\rho_2$, then (4.33) can be rewritten as

$$\rho_{F_t}(\tau_0) = (-1)^k (a_0(t))^{2(k+1)}. \tag{4.36}$$

Set

$$A_0(t) := \frac{1}{2}\operatorname{trace}(a_0(t)).$$

By Claim 2 and (4.21), we have that

$$A_0(t) = \frac{1}{2}(\psi^{-2}\overline{q(t)} + \psi^2 q(t)). \tag{4.37}$$

Letting $t \to 0$, we have $A_0(0) = \cos\{k\pi/(2(k+1))\}$ by (4.22). Then there exists a real analytic function $\theta_0 = \theta_0(t)$ such that

$$\cos\theta_0(t) = A_0(t) = \frac{1}{2}\operatorname{trace}(a_0(t)), \qquad \theta_0(0) = \frac{k\pi}{2(k+1)}. \tag{4.38}$$

Then the Cayley-Hamilton identity yields that $a_0(t)^2 = 2a_0(t)\cos\theta_0(t) - e_0$. Then by induction, one can prove the identity (purely algebraically)

$$(a_0)^m = \frac{\sin(m\theta_0)}{\sin\theta_0}a_0 - \frac{\sin((m-1)\theta_0)}{\sin\theta_0}e_0 \qquad (m = 1, 2, 3, \dots).$$

By (4.36), we have

$$\rho_{F_t}(\tau_0) = (-1)^k \left(\frac{\sin(2k+2)\theta_0}{\sin\theta_0}a_0 - \frac{\sin(2k+1)\theta_0}{\sin\theta_0}e_0\right).$$

Taking the trace of this, Lemma 4.14 yields

$$\cos\pi\nu_0 = \frac{\sin(2k+2)\theta_0}{\sin\theta_0}\cos\theta_0 - \frac{\sin(2k+1)\theta_0}{\sin\theta_0} = \cos(2k+2)\theta_0.$$

Hence

$$\pi\nu_0(t) \equiv \pm 2(k+1)\theta_0(t) \pmod{2\pi}.$$

Comparing both sides of this equation at $t = 0$, (4.38) implies

$$\pi\nu_0(t) = 2(k+1)\theta_0(t) \quad \text{or} \quad \pi\nu_0(t) = 2(k+1)(\pi - \theta_0(t)), \tag{4.39}$$

by real analyticity.

On the other hand, by Lemma 4.15, it holds that

$$\begin{aligned} -2(k+1)\pi i \begin{pmatrix} 1 & 0 \\ 0 & -1 \end{pmatrix} &= -\left.\frac{d\rho_{F_t}(\tau_0)^{-1}}{dt}\right|_{t=0} = \left.\frac{d\rho_{F_t}(\tau_0)}{dt}\right|_{t=0} \\ &= (-1)^k \left.\frac{d}{dt}\right|_{t=0} \left(\frac{\sin(2k+2)\theta_0}{\sin\theta_0}a_0 - \frac{\sin(2k+1)\theta_0}{\sin\theta_0}e_0\right), \end{aligned}$$

where we used the fact that $\rho_{F_0}(\tau_0) = e_0$. Since

$$\theta_0(0) = \frac{k\pi}{2k+2}, \quad \sin((2k+2)\theta_0(0)) = 0, \quad \cos((2k+2)\theta_0(0)) = (-1)^k,$$

by setting $\dot\theta_0(0) = d\theta_0/dt|_{t=0}$, we have that

$$\begin{aligned} &-2(k+1)\pi i \begin{pmatrix} 1 & 0 \\ 0 & -1 \end{pmatrix} \\ &\quad = (-1)^k \left.\frac{d}{dt}\right|_{t=0} \left(\frac{\sin(2k+2)\theta_0}{\sin\theta_0}a_0 - \frac{\sin\big((2k+2)\theta_0 - \theta_0\big)}{\sin\theta_0}e_0\right) \end{aligned}$$

$$= (-1)^k \left.\frac{d}{dt}\right|_{t=0} \left(\frac{\sin(2k+2)\theta_0}{\sin\theta_0} a_0 - \left(\frac{\sin(2k+2)\theta_0}{\sin\theta_0}\cos\theta_0 - \cos(2k+2)\theta_0 \right) e_0 \right)$$
$$= \frac{2k+2}{\sin\theta_0(0)} \left(a_0(0) - \cos\frac{k\pi}{2k+2} e_0 \right) \dot\theta_0(0)$$
$$= \frac{2k+2}{\sin\frac{k\pi}{2k+2}} \left(\overline{\sigma_3}\sigma_2 - \cos\frac{k\pi}{2k+2} e_0 \right) \dot\theta_0(0) = -2(k+1)i \begin{pmatrix} 1 & 0 \\ 0 & -1 \end{pmatrix} \dot\theta_0(0).$$

Thus, we have

$$\dot\theta_0(0) = e_0. \tag{4.40}$$

Then by (4.39), we have

$$\theta_0(t) = \frac{\pi\nu_0(t)}{2k+2}. \tag{4.41}$$

Similarly, if we set $a_\infty = \overline{\rho_1}\rho_3$, then (4.34) can be rewritten as

$$\rho_{F_t}(\tau_\infty) = (-1)^k (a_\infty(t))^{2(k+1)}. \tag{4.42}$$

Set

$$A_\infty(t) := \frac{1}{2}\operatorname{trace}(a_\infty(t)).$$

By Claim 2 and (4.21), we have that

$$A_\infty(t) = \frac{1}{2}(\overline{q(t)} + q(t)). \tag{4.43}$$

Letting $t \to 0$, we have $A_\infty(0) = \cos\{k\pi/(2k+2)\}$ by (4.22). Then there exists a real analytic function $\theta_\infty = \theta_\infty(t)$ such that

$$\cos\theta_\infty(t) = A_\infty(t) = \frac{1}{2}\operatorname{trace}(a_\infty(t)), \qquad \theta_\infty(0) = \frac{k\pi}{2k+2}. \tag{4.44}$$

Like as in the computation of $\theta_0(t)$, we have

$$\dot\theta_\infty(0) = -\pi, \qquad \theta_\infty(t) = \frac{\pi\nu_\infty(t)}{2k+2}. \tag{4.45}$$

By (4.37), (4.38), (4.43) and (4.44), we have that

$$\psi^2 q + \psi^{-2}\bar q = 2\cos\theta_0, \qquad q + \bar q = 2\cos\theta_\infty.$$

Hence

$$q(t) = \frac{-i}{\sin\frac{k\pi}{k+1}} \left(\cos\theta_0(t) - \psi^{-2}\cos\theta_\infty(t) \right)$$

and

$$q\bar q = \frac{1}{\sin^2\frac{k\pi}{k+1}} \left((\cos\theta_0)^2 + (\cos\theta_\infty)^2 - 2\left(\cos\frac{k\pi}{k+1}\right)\cos\theta_0\cos\theta_\infty \right).$$

Differentiating this twice using (4.40), (4.41) and (4.45), we have

$$q\bar q|_{t=0} = 1, \quad \left.\frac{d}{dt}\right|_{t=0} q\bar q = 0, \quad \left.\frac{d^2}{dt^2}\right|_{t=0} q\bar q = \frac{4(k+1)\pi}{k}\tan\frac{\pi k}{2k+2} > 0.$$

Thus, $(|q|^2 =) q\bar q > 1$ for t with sufficiently small absolute value, and by (4.21), $r_1 r_2 < 0$ holds. □

Proof of Proposition 4.13. Take $\iota(t)$ as in Claim 2. We set

$$\iota_1(t) = \iota(t)\begin{pmatrix} s(t) & 0 \\ 0 & 1/s(t) \end{pmatrix}, \qquad s(t) = \sqrt[4]{-r_1(t)/r_2(t)}.$$

Then by (1) of Proposition 4.12 and Claims 1 and 2, we have $\tilde{\rho}_{1,t,\iota_1(t)} = e_0 \in \mathrm{SU}_{1,1}$, $\tilde{\rho}_{2,t,\iota_1(t)} = \sigma_2 \in \mathrm{SU}_{1,1}$ and

$$\tilde{\rho}_{3,t,\iota_1(t)} = \begin{pmatrix} q(t) & \varepsilon i\sqrt{-r_1(t)r_2(t)} \\ -\varepsilon i\sqrt{-r_1(t)r_2(t)} & \overline{q(t)} \end{pmatrix} \in \mathrm{SU}_{1,1},$$

where $\varepsilon = 1$ (resp. -1) if $r_1(t) > 0$ (resp. $r_1(t) < 0$). By replacing $\iota(t)$ by $\iota_1(t)$, we have the conclusion. □

Thus, we obtain a one parameter family of CMC-1 faces $\{\hat{f}_{k,t}\}$ defined on M_k. When k is even, it induces $f_k \colon M'_k \to S^3_1$, where M'_k is the Riemann surface of genus $k/2$ as in Section 3.5, because $\{\tilde{\mu}_1, \tilde{\mu}_2, \tilde{\mu}_3\}$ generates the fundamental group of M'_k.

4.5. **Completeness and embeddedness.** Now, we have weakly complete CMC-1 faces $f_{k,t}$ for positive integers $k > 0$ and for $t \neq 0$ with sufficiently small absolute value. In this subsection, we shall prove completeness of $f_{k,t}$ and embeddedness of $f_{1,t}$ and $f_{2,t}$ for sufficiently small t, which shows the second part of Theorem B.

Proposition 4.16 (Completeness)**.** *For each positive integer k and for $t \neq 0$ with sufficiently small absolute value, the CMC-1 face $f_{k,t} \colon M_k \to S^3_1$ is complete, and each end is a regular elliptic end in the sense of* [12].

Proof. Since G is meromorphic at the ends, they are regular ends. Moreover, by (4.30) and (4.28), the end $(0,0)$ is g-regular non-integral elliptic in the sense of [12, Definition 3.3] because $\nu_0 \notin \pi\boldsymbol{Z}$. Then by Lemma E1 in [12], the singular set does not accumulate at the end, and hence the end $(0,0)$ is complete. Similarly, the end (∞,∞) is also complete. □

To show embeddedness, we shall look at the asymptotic behavior of the two ends of $f_{k,t}$. The ideal boundary of S^3_1 consists of two connected components:

$$\partial_+ S^3_1 = LC_+/\boldsymbol{R}_+ \qquad \text{and} \qquad \partial_- S^3_1 = LC_-/\boldsymbol{R}_+,$$

where LC_+ (resp. LC_-) denotes the positive (resp. negative) light cone in $\boldsymbol{R}^4_1$:

$$LC_\pm = \{(v_0, v_1, v_2, v_3) \in \boldsymbol{R}^4_1 \,;\, \pm v_0 > 0\},$$

see [12, Section 4].

Lemma 4.17. *For $t \neq 0$ with sufficiently small absolute value, the two ends of $f_{k,t}$ are asymptotic to the same point of the same connected component of the ideal boundary.*

Proof. Noticing $Q_t \to 0$ as $t \to 0$, (4.7) for (G, Q_t) implies that $S(g) \to S(G)$ as $t \to 0$. Since $G(0,0) = G(\infty,\infty) = \infty$ (see Table 1 in Section 3), this implies that $|g| - 1$ has the same sign at $(0,0)$ and (∞,∞). In particular, one can choose g such that $|g| > 1$ on neighborhoods of $(0,0)$ and (∞,∞). Then by Proposition 4.2 in [12], $f_{k,t}$ converges to $\partial_- S^3_1$ at the two ends. Moreover, since $G(0,0) = G(\infty,\infty)$, the proof of [12, Proposition 4.2] implies that both of the ends converge to the same point of $\partial_- S^3_1$. □

Proposition 4.18. *For $t \neq 0$ with sufficiently small absolute value, the CMC-1 face $f_{k,t}$ is embedded if and only if $k = 1$ or 2.*

Proof. By Table 1 in Section 3, G has poles of order k at $(0,0)$ and (∞,∞) in $\overline{M}_k$. Then there exists a complex coordinate ζ of $\overline{M}_k$ around $(0,0)$ such that $G = \zeta^{-k}$. On the other hand, by (4.30), g is represented as

$$g = \zeta^{-\nu_0}\big(\alpha + o(1)\big) \qquad \alpha \in \boldsymbol{R} \setminus \{0\},$$

where $\nu_0 > 0$ is as in (4.28), since we can replace the secondary Gauss map g by $1/g$. Then by Small's formula [12, Equation (1.10)] (see also [21]), the holomorphic lift F is expressed as

$$F = \frac{1}{2\sqrt{k\nu_0}} \begin{pmatrix} \zeta^{\frac{-k+\nu_0}{2}}(k+\nu_0)\left(\dfrac{-1}{\sqrt{\alpha}} + o(1)\right) & \zeta^{\frac{-k-\nu_0}{2}}(k-\nu_0)\left(\dfrac{1}{\sqrt{\alpha}} + o(1)\right) \\ \zeta^{\frac{k+\nu_0}{2}}(k-\nu_0)\left(\sqrt{\alpha} + o(1)\right) & \zeta^{\frac{k-\nu_0}{2}}(k+\nu_0)\left(-\sqrt{\alpha} + o(1)\right) \end{pmatrix},$$

where $o(\cdot)$ denotes a higher order term. Hence the coordinate functions of $\hat{f}_{k,t} = Fe_3F^*$ as in (4.1) are expressed as

$$\begin{aligned} x_0 &= -r^{-(k+\nu_0)}\big(\alpha_0 + o(1)\big), \\ x_3 &= -r^{-(k+\nu_0)}\big(\alpha_0 + o(1)\big), \quad x_1 + ix_2 = r^{-\nu_0}e^{ik\theta}\alpha_1\big(1 + o(1)\big), \end{aligned}$$

where α_0, α_1 are positive real numbers and $\zeta = re^{i\theta}$. Hence $x_0 \to -\infty$ as $r \to 0$ and

$$x_1 + ix_2 = C_1 e^{ik\theta} x_0^{\frac{\nu_0}{k+\nu_0}}\big(1 + o(1)\big), \qquad x_3 = x_0\big(1 + o(1)\big),$$

where C_1 is a non-zero constant. Similarly, the end (∞,∞) is expressed as

$$x_1 + ix_2 = C_2 e^{ik\theta} x_0^{\frac{\nu_\infty}{k+\nu_\infty}}\big(1 + o(1)\big), \qquad x_3 = x_0\big(1 + o(1)\big),$$

where ν_∞ is as in (4.29) and C_2 is a non-zero constant. Since $\nu_0 \neq \nu_\infty$, these two ends do not intersect each other in sufficiently small neighborhood of the ends. Moreover, each end has no self intersection if and only if $k = 1$, or $k = 2$ (notice that M_2 is a double cover of M_2'). □

Appendix A. Reflections and fundamental groups

In this appendix, we review the properties of the fundamental group and reflections on Riemann surfaces, which were used in Section 4.

A.1. **Properties of reflections.** Let M be a connected Riemann surface and fix a base point $o \in M$. We denote the set of continuous paths starting at o by

$$C_o(M) := \{\gamma\colon [0,1] \to M;\ \gamma \text{ is continuous and } \gamma(0) = o\}.$$

We denote by $[\gamma]$ the homotopy class containing $\gamma \in C_o(M)$. Then the universal covering space $\widetilde{M}$ can be canonically identified with the quotient space $\{[\gamma]\,;\,\gamma \in C_o(M)\}$, and the covering projection is given by

$$\pi : \widetilde{M} \ni [\gamma] \longmapsto \gamma(1) \in M.$$

When two paths $\gamma_j\colon [0,1] \to M$ $(j = 1,2)$ satisfy $\gamma_1(1) = \gamma_2(0)$, we denote by $\gamma_1 * \gamma_2$ the path obtained by joining γ_1 and γ_2 as follows:

$$\gamma_1 * \gamma_2(u) := \begin{cases} \gamma_1(2u) & \text{if } u \in [0,1/2], \\ \gamma_2(2u-1) & \text{if } u \in [1/2,1]. \end{cases} \tag{A.1}$$

We denote the set of loops at o by $L_o(M) := \{\gamma \in C_o(M)\,;\, \gamma(1) = o\}$. The *fundamental group* $\pi_1(M)$ is the set of homotopy classes of $L_o(M)$ with group multiplication induced from (A.1), which acts on $\widetilde{M}$ as *covering transformations*, as follows:

$$\tau\colon \widetilde{M} \ni [\gamma] \longrightarrow [\gamma_1 * \gamma] \in \widetilde{M} \qquad \big(\tau = [\gamma_1] \in \pi_1(M)\big), \tag{A.2}$$

where $\gamma_1 \in L_o(M)$ and $\gamma \in C_o(M)$.

An orientation-reversing conformal involution $\mu : M \to M$ is called a *reflection* of M. In this section, we want to define a reflection of $\widetilde{M}$ as a lift of μ. Let $P_\mu\colon [0,1] \to M$ be a path starting from o and ending at $\mu(o)$. We suppose that P_μ is μ-invariant, that is,

$$\mu \circ P_\mu(u) = P_\mu(1-u) = {P_\mu}^{-1}(u) \qquad (u \in [0,1]). \tag{A.3}$$

Now we define a map $\tilde{\mu} : \widetilde{M} \longrightarrow \widetilde{M}$ by

$$\tilde{\mu}([\gamma]) := [P_\mu * (\mu \circ \gamma)], \tag{A.4}$$

which is called the *lift* of μ with respect to P_μ. Then the following assertion holds:

Lemma A.1. *The lift $\tilde{\mu}$ is an involution of $\widetilde{M}$.*

Proof. By (A.3), $P(\mu)^{-1} * P(\mu)$ is homotopic to the constant map $[0,1] \ni u \mapsto o \in M$. Then $\tilde{\mu} \circ \tilde{\mu}([\gamma]) = \tilde{\mu}([P_\mu * (\mu \circ \gamma)]) = [P_\mu^{-1} * P_\mu * (\mu \circ \mu \circ \gamma)] = [\gamma]$. □

We now prove the following:

Proposition A.2. *Let $\mu_1, \ldots, \mu_{2r}$ be a sequence of reflections on M, and take the lift $\tilde{\mu}_j$ of μ_j with respect to the curve P_{μ_j} for each $j = 1, \ldots, 2r$. Suppose that $\mu_1 \circ \cdots \circ \mu_{2r}$ is the identity map id_M on M. Then*

$$\tilde{\mu}_1 \circ \cdots \circ \tilde{\mu}_{2r} : \widetilde{M} \longrightarrow \widetilde{M}$$

gives a covering transformation on the universal covering $\widetilde{M}$ of M which corresponds to the loop

$$P_{\mu_1} * (\mu_1 \circ P_{\mu_2}) * (\mu_1 \circ \mu_2 \circ P_{\mu_3}) * \cdots * (\mu_1 \circ \mu_2 \circ \cdots \circ \mu_{2r-1} \circ P_{\mu_{2r}}).$$

We call $\tilde{\mu}_1 \circ \cdots \circ \tilde{\mu}_{2r}$ the covering transformation associated with $\mu_1, \ldots, \mu_{2r}$.

Proof of Proposition A.2. For the sake of simplicity, we write $P_j := P_{\mu_j}$. Then for each $\gamma \in C_o(M)$, it holds that

$$\tilde{\mu}_1 \circ \cdots \circ \tilde{\mu}_r([\gamma]) = [P_1 * (\mu_1 \circ P_2) * \cdots * (\mu_1 \circ \cdots \circ \mu_{2r-1} \circ P_{2r}) * (\mu_1 \circ \cdots \circ \mu_{2r} \circ \gamma)].$$

Since $\mu_1 \circ \cdots \circ \mu_{2r} = \mathrm{id}_M$, we have the conclusion. □

Remark A.3. Proposition A.2 gives a method to explicitly write down the isomorphism between the covering transformation group and the fundamental group $\pi_1(M)$.

A.2. **A certain analytic property of reflections.** Let G be a meromorphic function and Q a holomorphic 2-differential on the Riemann surface M. Such a pair (G, Q) is called *admissible* if

$$ds^2_{\#} := \bigl(1 + |G|^2\bigr)^2 \left|\frac{Q}{dG}\right|^2 \tag{A.5}$$

gives a (positive definite) Riemannian metric on M.

Let $\pi\colon \widetilde{M} \to M$ be the universal covering as in Appendix A.1, and let $\tilde{o} \in \widetilde{M}$ be the point corresponding to the constant path at $o \in M$ (then $\pi(\tilde{o}) = o$ holds). For an admissible pair (G, Q) on M, we define

$$\widetilde{G} := G \circ \pi, \qquad \widetilde{Q} := Q \circ \pi.$$

Then $(\widetilde{G}, \widetilde{Q})$ is an admissible pair on $\widetilde{M}$ which is invariant under the covering transformations. Consider the following ordinary differential equation

$$dFF^{-1} = \Psi, \qquad \Psi := \begin{pmatrix} \widetilde{G} & -\widetilde{G}^2 \\ 1 & -\widetilde{G} \end{pmatrix} \frac{\widetilde{Q}}{d\widetilde{G}} \tag{A.6}$$

with the initial condition

$$F(\tilde{o}) = a \in \mathrm{SL}_2\boldsymbol{C}. \tag{A.7}$$

Proposition A.4. *For each $a \in \mathrm{SL}_2\boldsymbol{C}$, there exists a unique holomorphic null immersion $F\colon \widetilde{M} \to \mathrm{SL}_2\boldsymbol{C}$ satisfying* (A.6) *and* (A.7)*. For such an immersion F, there exists a representation $\rho_F\colon \pi_1(M) \to \mathrm{SL}_2\boldsymbol{C}$ such that*

$$F \circ \tau = F\rho_F(\tau)^{-1} \qquad \bigl(\tau \in \pi_1(M)\bigr),$$

where τ is considered as a covering transformation. Moreover, we set a holomorphic function g on $\widetilde{M}$ as $g = -dF_{12}/dF_{11} = -dF_{22}/dF_{21}$ (that is, g is the secondary Gauss map) where $F = (F_{ij})$. Then it satisfies $g \circ \tau = \rho_F(\tau) \star g$, where $\star$ denotes the Möbius transformation:

$$a \star g := \frac{a_{11}g + a_{12}}{a_{21}g + a_{22}} \qquad \bigl(a = (a_{ij}) \in \mathrm{SL}_2\boldsymbol{C}\bigr). \tag{A.8}$$

We call ρ_F the *representation associated to* F.

Proof of Proposition A.4. By admissibility, Ψ is an $\mathfrak{sl}_2\boldsymbol{C}$-valued holomorphic one-form. Then the existence and uniqueness of F follows. Since Ψ is τ-invariant, $F \circ \tau$ is also a solution of (A.6). Hence the existence of ρ_F follows. The final assertion can be shown directly. □

Let μ be a reflection on M. Then an admissible pair (G, Q) is said to be *μ-invariant* if

$$ds^2_{\#} \circ \mu = ds^2_{\#} \qquad \text{and} \qquad \overline{Q \circ \mu} = Q \tag{A.9}$$

hold, where $ds^2_{\#}$ is the metric as in (A.5).

Lemma A.5 (See [27, Lemma 4.2])**.** *Let (G, Q) be an μ-invariant admissible pair on M, where μ is a reflection of M whose fixed point set is not empty. Then there exists a matrix $\sigma(\mu)$ such that*

$$\overline{G \circ \mu} = \sigma(\mu) \star G, \tag{A.10}$$

where $\star$ denotes the Möbius transformation in (A.8)*. Moreover, such a matrix $\sigma(\mu)$ is unique up to $\pm$-ambiguity, and is written in the following form*:

$$\sigma(\mu) = \begin{pmatrix} q_\mu & is_\mu \\ is_\mu & \overline{q_\mu} \end{pmatrix}, \quad \left(q_\mu \in \boldsymbol{C},\ s_\mu \in \boldsymbol{R},\ |q_\mu|^2 + (s_\mu)^2 = 1\right).$$

In particular $\overline{\sigma(\mu)}\sigma(\mu) = e_0$ holds, where e_0 is the identity matrix.

Proof. By (A.9), the pull-back $ds^2_{FS} := 4|dG|^2/(1+|G|^2)^2$ of the Fubini-Study metric of $\boldsymbol{C} \cup \{\infty\}$ by G is μ-invariant. Hence $\overline{G \circ \mu}$ is an orientation-preserving developing map of ds^2_{FS}, as well as G. Then there exists $\sigma \in \mathrm{SU}_2$ such that $\overline{G \circ \mu} = \sigma \star G$. Since $G = G \circ \mu \circ \mu = \overline{\sigma}\sigma \star G$, $\bar{\sigma}\sigma = \pm e_0$ holds. If $\bar{\sigma}\sigma = -e_0$ holds,

$$\sigma = \pm \begin{pmatrix} 0 & -1 \\ 1 & 0 \end{pmatrix}$$

because $\sigma \in \mathrm{SU}_2$. In this case, for a fixed point z of μ,

$$\overline{G(z)} = \overline{G \circ \mu(z)} = \sigma \star G(z) = -\frac{1}{G(z)}, \qquad \text{that is,} \quad |G(z)|^2 = -1$$

holds, which is impossible. Then $\overline{\sigma}\sigma = e_0$, and by a direct calculation we have the conclusion. □

Theorem A.6. *Let (G, Q) be a μ-invariant admissible pair satisfying* (A.10)*, and take a lift $\tilde{\mu}\colon \widetilde{M} \to \widetilde{M}$ as in* (A.4)*. Assume $F : \widetilde{M} \to \mathrm{SL}_2\boldsymbol{C}$ satisfies* (A.6)*. Then there exists $\rho(\tilde{\mu}) \in \mathrm{SL}_2\boldsymbol{C}$ such that*

$$\overline{F \circ \tilde{\mu}} = \sigma(\mu) F \rho(\tilde{\mu})^{-1}, \tag{A.11}$$

where $\sigma(\mu)$ is as in Lemma A.5. Moreover, $\rho(\tilde{\mu})$ is written as

$$\rho(\tilde{\mu}) = \begin{pmatrix} q & is_1 \\ is_2 & \overline{q} \end{pmatrix} \qquad \left(q \in \boldsymbol{C},\ s_j \in \boldsymbol{R}\ (j = 1, 2),\ |q|^2 + s_1 s_2 = 1\right). \tag{A.12}$$

Proof. By (A.9) and Lemma A.5, $\overline{\Psi \circ \mu} = \sigma\Psi\sigma^{-1}$ holds, where $\sigma = \sigma(\mu)$. Then

$$d(\sigma F)(\sigma F)^{-1} = \sigma\Psi\sigma^{-1} = \overline{\Psi \circ \mu} = d\overline{(F \circ \tilde{\mu})}(\overline{F \circ \tilde{\mu}})^{-1},$$

which implies that $\sigma^{-1}F$ and $\overline{F \circ \tilde{\mu}}$ satisfy the same equation. Thus, there exists $\rho = \rho(\tilde{\mu}) \in \mathrm{SL}_2\boldsymbol{C}$ such that $\overline{F \circ \tilde{\mu}} = \sigma F \rho^{-1}$. Since $\tilde{\mu}$ is an involution and $\overline{\sigma}\sigma = e_0$, $\overline{\rho}\rho = e_0$ holds. Noticing $\rho \in \mathrm{SL}_2\boldsymbol{C}$, we have (A.12). □

Finally, we write a representation ρ_F as in Proposition A.4 of the fundamental group in terms of reflections.

Definition A.7. Let $\mu_1, \ldots, \mu_N$ be mutually distinct reflections on M and take the lift $\tilde{\mu}_j$ of μ_j for $j = 1, \ldots, N$ as in (A.4). If each covering transformation $\tau \in \pi_1(M)$ has an expression

$$\tau = \tilde{\mu}_{i_1} \circ \cdots \circ \tilde{\mu}_{i_{2r}}, \tag{A.13}$$

then $\{\tilde{\mu}_1, \ldots, \tilde{\mu}_N\}$ is called a *generator* of $\pi_1(M)$.

We now fix a generator $\{\tilde{\mu}_1, \ldots, \tilde{\mu}_N\}$ and take an admissible pair (G, Q) on M which is μ_j-invariant for each $j = 1, \ldots, N$. Choose $\sigma(\mu_j)$ as in Lemma A.5 for each $j = 1, \ldots, N$.

Lemma A.8. *If a covering transformation $\tau \in \pi_1(M)$ is written as in* (A.13) *in terms of a generator,*

$$\overline{\sigma(\mu_{i_1})}\sigma(\mu_{i_2})\dots\overline{\sigma(\mu_{i_{2r-1}})}\sigma(\mu_{i_{2r}})$$

is equal to e_0 or $-e_0$.

Proof. Since $\mu_{i_1}\circ\cdots\circ\mu_{i_{2r}} = \mathrm{id}_M$, we have

$$G = G\circ\mu_{i_1}\circ\cdots\circ\mu_{i_{2r}} = \left(\overline{\sigma(\mu_{i_1})}\sigma(\mu_{i_2})\dots\overline{\sigma(\mu_{i_{2r-1}})}\sigma(\mu_{i_{2r}})\right)\star G.$$

Thus, we have the conclusion. □

Then, by the definition of the representation ρ_F in Proposition A.4, we have

Proposition A.9. *Under the situations above, we have*

$$\rho_F(\tau) = \left(\overline{\sigma(\mu_{i_1})}\sigma(\mu_{i_2})\dots\overline{\sigma(\mu_{i_{2r-1}})}\sigma(\mu_{i_{2r}})\right)\left(\overline{\rho(\tilde{\mu}_{i_1})}\rho(\tilde{\mu}_{i_2})\dots\overline{\rho(\tilde{\mu}_{i_{2r-1}})}\rho(\tilde{\mu}_{i_{2r}})\right).$$

Note that the $\pm$-ambiguity of $\sigma(\mu_j)$ does not affect this expression, because if one were to choose $-\sigma(\mu_j)$ instead of $\sigma(\mu_j)$, $\rho(\tilde{\mu}_j)$ changes to $-\rho(\tilde{\mu}_j)$.

Hence we have

Theorem A.10. *Let M be a Riemann surface with reflections $\{\mu_1,\dots,\mu_N\}$, and assume its lift $\{\tilde{\mu}_1,\dots,\tilde{\mu}_N\}$ is a generator of $\pi_1(M)$. Take an admissible pair (G,Q) on M which is μ_j-invariant for each $j=1,\dots,N$, and let F be a solution of* (A.6)*, ρ_F a representation as in Proposition A.4, and $\rho(\tilde{\mu}_j)$ $(j=1,\dots,N)$ as in* (A.11)*. Then, if $\rho(\tilde{\mu}_j)\in \mathrm{SU}_{1,1}$ holds for all $j=1,\dots,N$, the image $\rho_F(\pi_1(M))$ lies in $\mathrm{SU}_{1,1}$.*

References

[1] L. Alías, R. M. B. Chaves and P. Mira, *Björling problem for maximal surfaces in Lorentz-Minkowski space*, Math. Proc. Cambridge Philos. Soc., **134** (2003), no. 2, 289–316.

[2] E. Calabi, *Examples of Bernstein problems for some nonlinear equations*, Proc. Symp. Pure Math., **15** (1970), 223–230.

[3] S.-Y. Cheng and S.-T. Yau, *Maximal space-like hypersurfaces in the Lorentz-Minkowski spaces*, Ann. of Math., **104** (1976), 407–419.

[4] F. J. M. Estudillo and A. Romero, *Generalized maximal surfaces in Lorentz- Minkowski space L^3*, Math. Proc. Camb. Phil. Soc., **111** (1992), 515–524.

[5] I. Fernández, *The number of conformally equivalent maximal graphs*, preprint, arXiv:0903.2950.

[6] I. Fernández and F. J. López, *Periodic maximal surfaces in the Lorentz-Minkowski space $\mathbb{L}^3$*, Math. Z., **256** (2007), 573–601.

[7] I. Fernández, F. J. López, and R. Souam, *The space of complete embedded maximal surfaces with isolated singularities in 3-dimensional Lorentz-Minkowski space L^3*, Math. Ann., **332** (2005), 605–643.

[8] S. Fujimori, *Spacelike CMC 1 surfaces with elliptic ends in de Sitter 3-Space*, Hokkaido Math. J., **35** (2006), 289–320.

[9] S. Fujimori, *Spacelike CMC 1 surfaces of genus 1 with two ends in de Sitter 3-space*, Kyushu J. Math., **61** (2007), 1–20.

[10] S. Fujimori and F. J. López, *Nonorientable maximal surfaces in the Lorentz-Minkowski 3-space*, preprint, arXiv:0905.2113.

[11] S. Fujimori and W. Rossman, *Higher genus mean curvature 1 catenoids in hyperbolic and de Sitter 3-spaces*, preprint, arXiv:0904.3988.

[12] S. Fujimori, W. Rossman, M. Umehara, K. Yamada and S.-D. Yang, *Spacelike mean curvature one surfaces in de Sitter 3-space*, Comm. Anal. Geom., **17** (2009), 383–427.

[13] S. Fujimori, W. Rossman, M. Umehara, K. Yamada and S.-D. Yang, *Triply periodic maximal surfaces in Minkowski 3-space*, in preparation.

[14] S. Fujimori, K. Saji, M. Umehara and K. Yamada, *Singularities of maximal surfaces*, Math. Z., **259** (2008), 827–848.
[15] T. Imaizumi, *Maximal surfaces with simple ends*, Kyushu J. Math., **58** (2004), 59–70.
[16] T. Imaizumi and S. Kato, *Flux of simple ends of maximal surfaces in* $\boldsymbol{R}^{2,1}$ Hokkaido Math. J., **37** (2008), 561–610.
[17] S. Kato, personal communication.
[18] O. Kobayashi, *Maximal surfaces in the* 3*-dimensional Minkowski space* $\mathbb{L}^3$, Tokyo J. Math., **6** (1983), 297–309.
[19] O. Kobayashi, *Maximal surfaces with conelike singularities*, J. Math. Soc. Japan, **36** (1984), 609–617.
[20] M. Kokubu and M. Umehara, *Orientability of linear Weingarten surfaces, spacelike CMC*-1 *surfaces and maximal surfaces.* preprint, arXiv:0907.2284.
[21] M. Kokubu, M. Umehara and K. Yamada, *An elementary proof of Small's formula for null curves in* $\mathrm{PSL}(2,\boldsymbol{C})$ *and an analogue for Legendrian curves in* $\mathrm{PSL}(2,\boldsymbol{C})$, Osaka J. of Math., **40** (2003), 697–715.
[22] Y. W. Kim and S.-D. Yang, *A family of maximal surfaces in Lorentz-Minkowski three-space*, Proc. Amer. Math. Soc., **134** (2006), 3379–3390.
[23] Y. W. Kim and S.-D. Yang, *Prescribing singularities of maximal surfaces via a singular Björling representation formula*, J. Geom. Phys., **57** (2007), no. 11, 2167–2177.
[24] F. J. López F.J., R. López and R. Souam, *Maximal surfaces of Riemann type in Lorentz-Minkowski space* L^3, Michigan J. Math., **47** (2000), 469–497.
[25] F. Martín, M. Umehara and K. Yamada, *Complete bounded null curves immersed in* $\boldsymbol{C}^3$ *and* $\mathrm{PSL}(2,\boldsymbol{C})$, Calc. Var. Partial Differential Equations, **36** (2009), 119–139.
[26] F. Martín, Umehara and K. Yamada, *Complete bounded holomorphic curves immersed in* $\boldsymbol{C}^2$ *with arbitrary genus*, Proc. Amer. Math. Soc., **137** (2009), no. 10, 3437–3450.
[27] W. Rossman, M. Umehara and K. Yamada, *Irreducible constant mean curvature* 1 *surfaces in hyperbolic space with positive genus*, Tôhoku Math. J., **49** (1997), 449–484.
[28] K. Sato, *Construction of higher genus minimal surfaces with one end and finite total curvature*, Tôhoku Math. J., **48** (1996), 229–446.
[29] R. Schoen, *Uniqueness, symmetry and embeddedness of minimal surfaces*, J. Differential Geometry, **18** (1983), 791–809.
[30] M. Umehara and K. Yamada, *A parametrization of the Weierstrass formulae and perturbation of some complete minimal surfaces of* $\mathbf{R}^3$ *into the hyperbolic* 3*-space*, J. für reine u. angew. Math., **432** (1992), 93–116.
[31] M. Umehara and K. Yamada, *Duality on CMC*-1 *surfaces in hyperbolic* 3*-space, and hyperbolic analogue of the Osserman inequality*, Tsukuba J. Math., **21** (1997), 229–237.
[32] M. Umehara and K. Yamada, *Maximal surfaces with singularities in Minkowski space*, Hokkaido Math. J., **35** (2006), 13–40.
[33] M. Umehara and K. Yamada, *Applications of a completeness lemma in minimal surface theory to various classes of surfaces*, preprint, arXiv:0909.1128.

Department of Mathematics, Fukuoka University of Education, Munakata, Fukuoka 811-4192, Japan
E-mail address: fujimori@fukuoka-edu.ac.jp

Department of Mathematics, Faculty of Science, Kobe University, Rokko, Kobe 657-8501, Japan
E-mail address: wayne@math.kobe-u.ac.jp

Department of Mathematics, Graduate School of Science, Osaka University, Toyonaka, Osaka 560-0043, Japan
E-mail address: umehara@math.sci.osaka-u.ac.jp

Department of Mathematics, Tokyo Institute of Technology, O-okayama, Meguro, Tokyo 152-8551, Japan
E-mail address: kotaro@math.titech.ac.jp

Department of Mathematics, Korea University, Seoul 136-701, Korea
E-mail address: sdyang@korea.ac.kr